Demonstrating Ignition Hydrodynamic Equivalence in Cryogenic DT Implosions on OMEGA

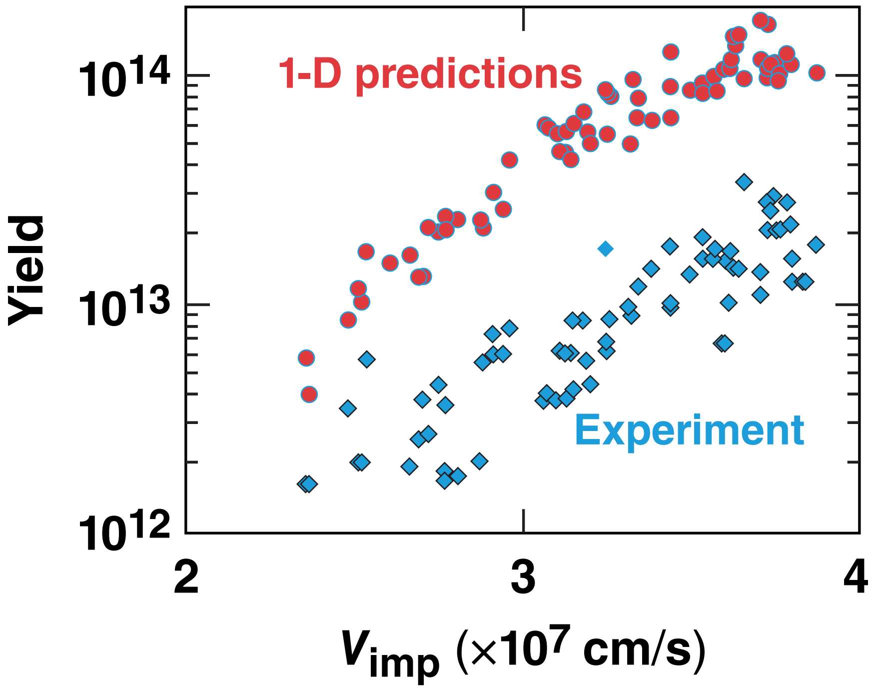

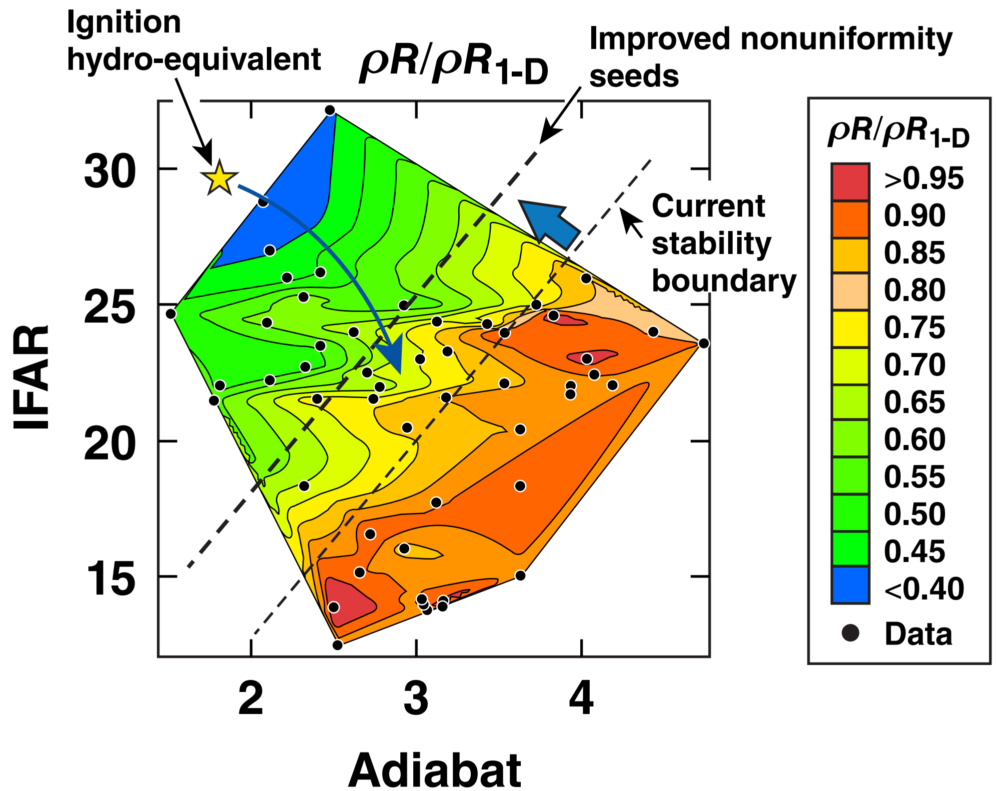

V. N. Goncharov
University of Rochester
Laboratory for Laser Energetics

Omega Laser Facility
Users Group Workshop
Rochester, NY
23–25 April 2014

Summary

The performance degradation of OMEGA cryogenic implosions is understood in terms of unshocked shell mass at stagnation

- Yields in excess of 3.4×10^{13} [yield-over-clean (YOC) ~ 35%] and ion temperatures up to 4 keV were measured in cryogenic implosions with $V_{imp} \sim 3.8 \times 10^7$ cm/s
- Performance degradation in moderate-adiabat ($\alpha \sim 4$) implosions is fully understood by 2-D *DRACO* simulations
- Shells in lower-adiabat implosions ($\alpha \sim 2.5$) break up during acceleration, leading to an increased hot-spot mass and reduced convergence
- The unshocked mass at peak compression determines the impact of the ablator mix

Improving shell stability and mitigating cross-beam energy transfer (CBET) are required to demonstrate ignition hydrodynamic scaling on OMEGA.

TC10247c

Collaborators

T. C. Sangster, R. Betti, T. R. Boehly, T. J. B. Collins, R. S. Craxton, J. A. Delettrez, D. H. Edgell, R. Epstein, C. J. Forrest, D. H. Froula, V. Yu. Glebov, D. R. Harding, S. X. Hu, I. V. Igumenshchev, R. Janezic, J. H. Kelly, T. J. Kessler, T. Z. Kosc, S. J. Loucks, J. A. Marozas, F. J. Marshall, A. V. Maximov, R. L. McCrory, P. W. McKenty, D. D. Meyerhofer, D. T. Michel, J. F. Myatt, R. Nora, P. B. Radha, S. P. Regan, W. Seka, W. T. Shmayda, R. W. Short, A. Shvydky, S. Skupsky, C. Sorce, C. Stoeckl, and B. Yaakobi

Laboratory for Laser Energetics
University of Rochester

J. A. Frenje, M. Gatu Johnson, and R. D. Petrasso

Plasma Science and Fusion Center, MIT

D. T. Casey

Lawrence Livermore National Laboratory

Direct-drive target performance is optimized by varying implosion velocity, in-flight aspect ratio (IFAR), fuel adiabat, and ablator material

- V_{imp} and IFAR are controlled by varying the ablator (7.5 to 12 μm) and fuel thickness (40 to 66 μm)

Adiabat
$\alpha = P/P_{Fermi}$

IFAR = shell radius/ shell thickness

Adiabat and IFAR are controlled by pulse shaping

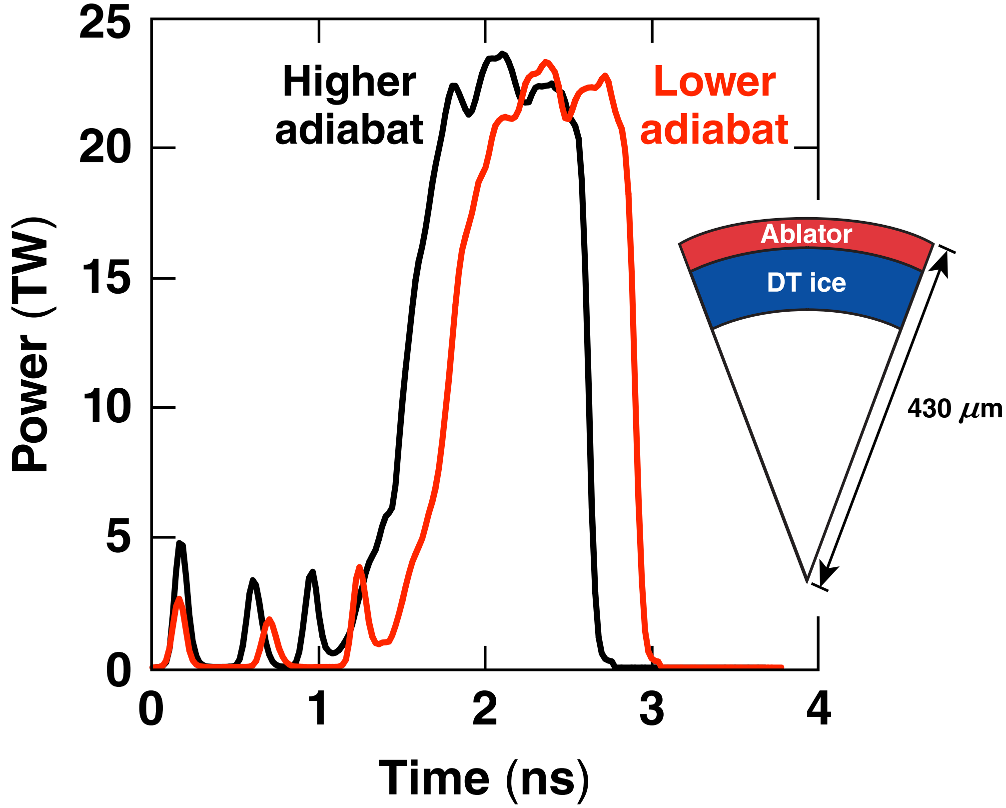

TC10248h

One-dimensional dynamics are verified using self-emission, bang time, and scattered-light measurements

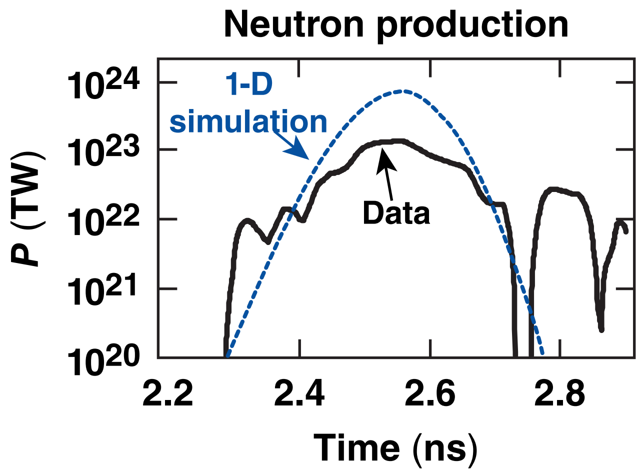

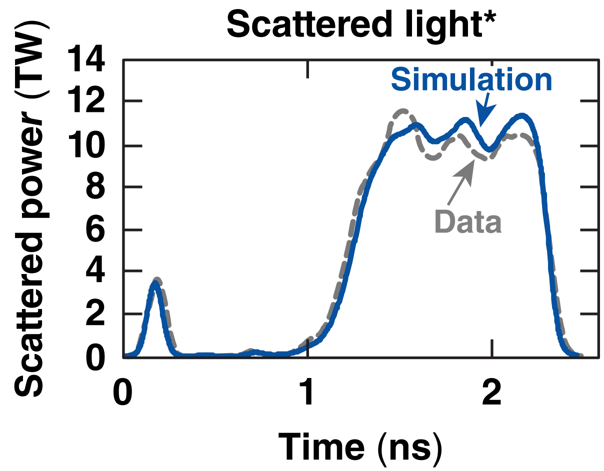

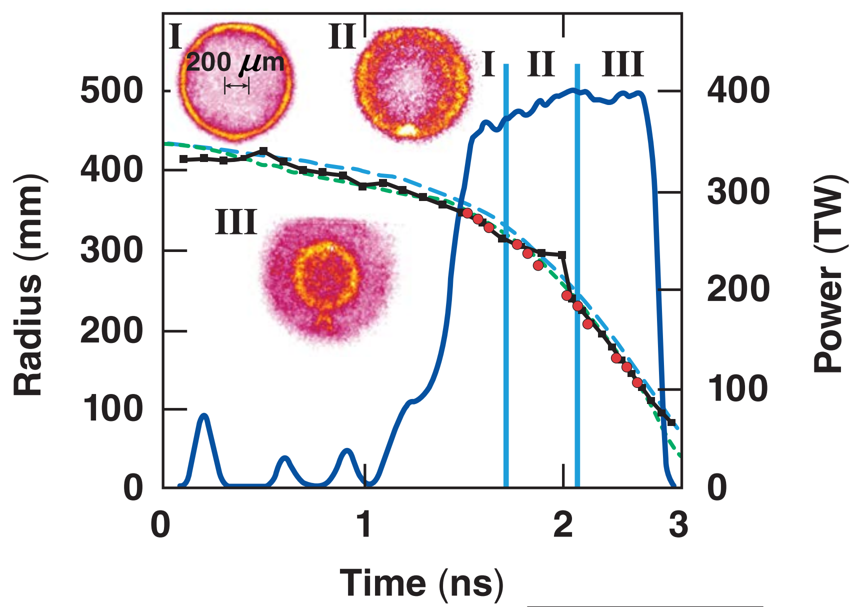

TC10789c

*W. Seka *et al*., Phys. Plasmas 15, 056312 (2008).

Target yield has a strong dependence on implosion velocity

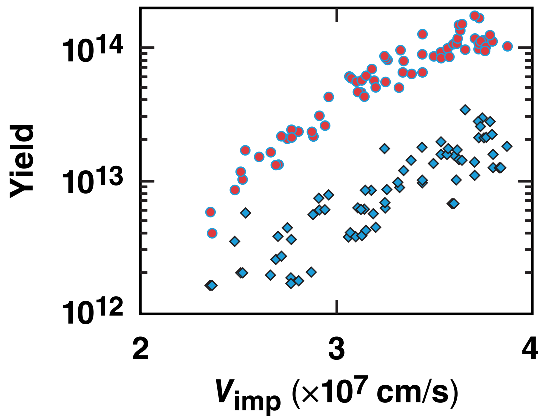

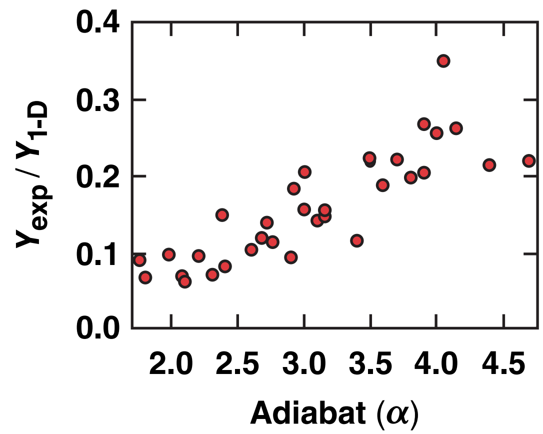

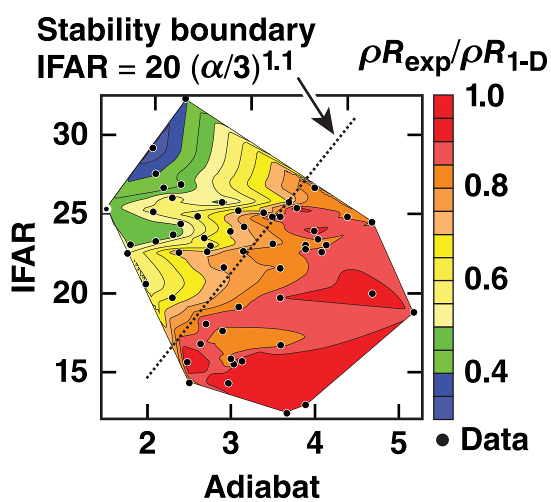

Target Performance

The maximum hot-spot pressure can be estimated using the measured neutron production rate

$$\frac{dN}{dt} \sim n^2 \langle \sigma v \rangle V_{hs} \sim p_{hs}^2 V_{hs} T^{2.5}$$

$$p_{hs} V_{hs}^{5/3} = \text{const}$$

$$\frac{dN}{dt} \sim p_{hs}^{7/5} T^{2.5}$$

Measured

$$p_{exp} \simeq p_{sim} \left(\frac{T_{exp}}{T_{sim}}\right)^{-1.8} \left(\frac{\dot{N}_{exp}}{\dot{N}_{sim}}\right)^{0.7}$$

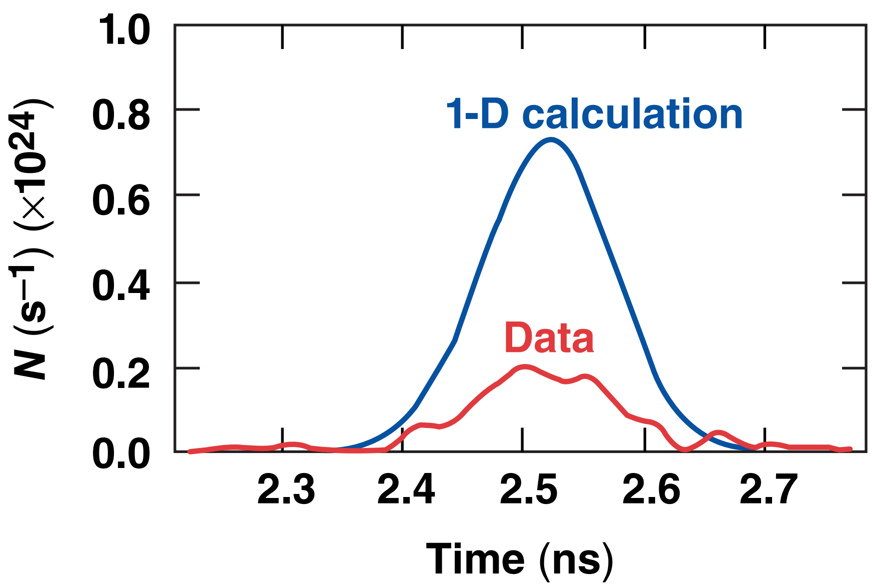

Pressures up to ~40 Gbar are inferred in $\alpha \sim 4$ implosions

Central pressure

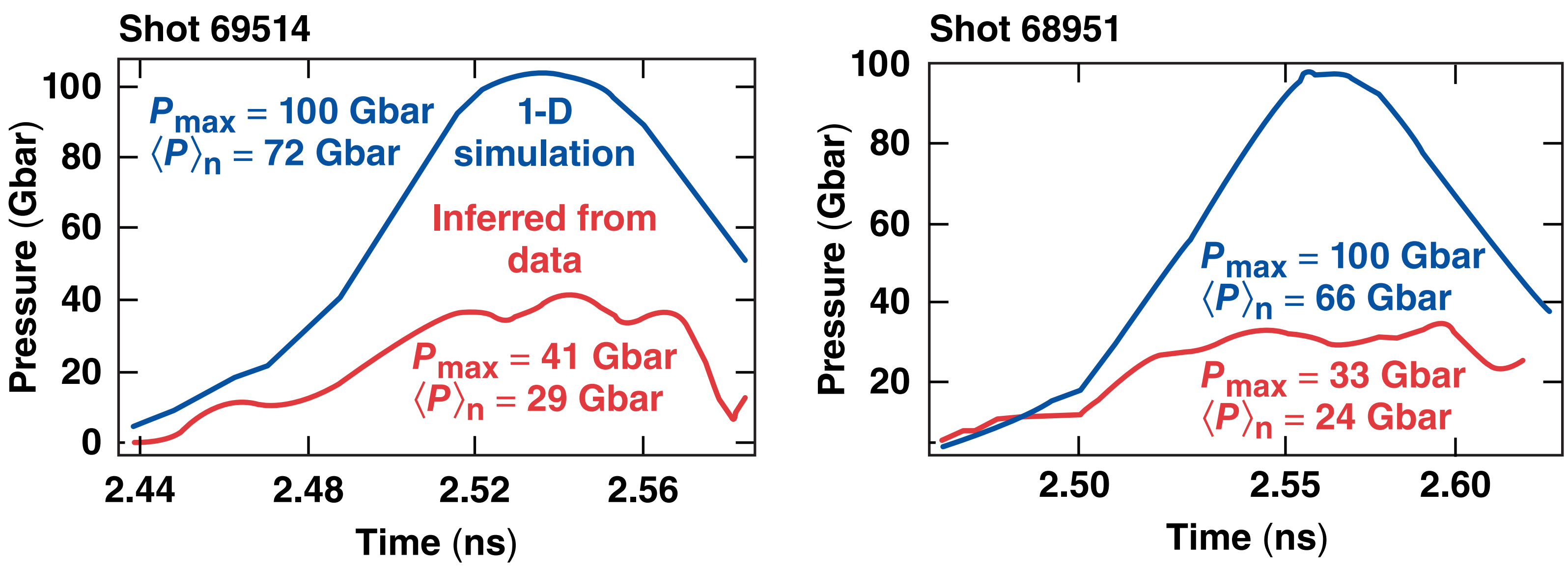

TC10957

Pressure is significantly reduced in low-adiabat (α < 2.5) implosions

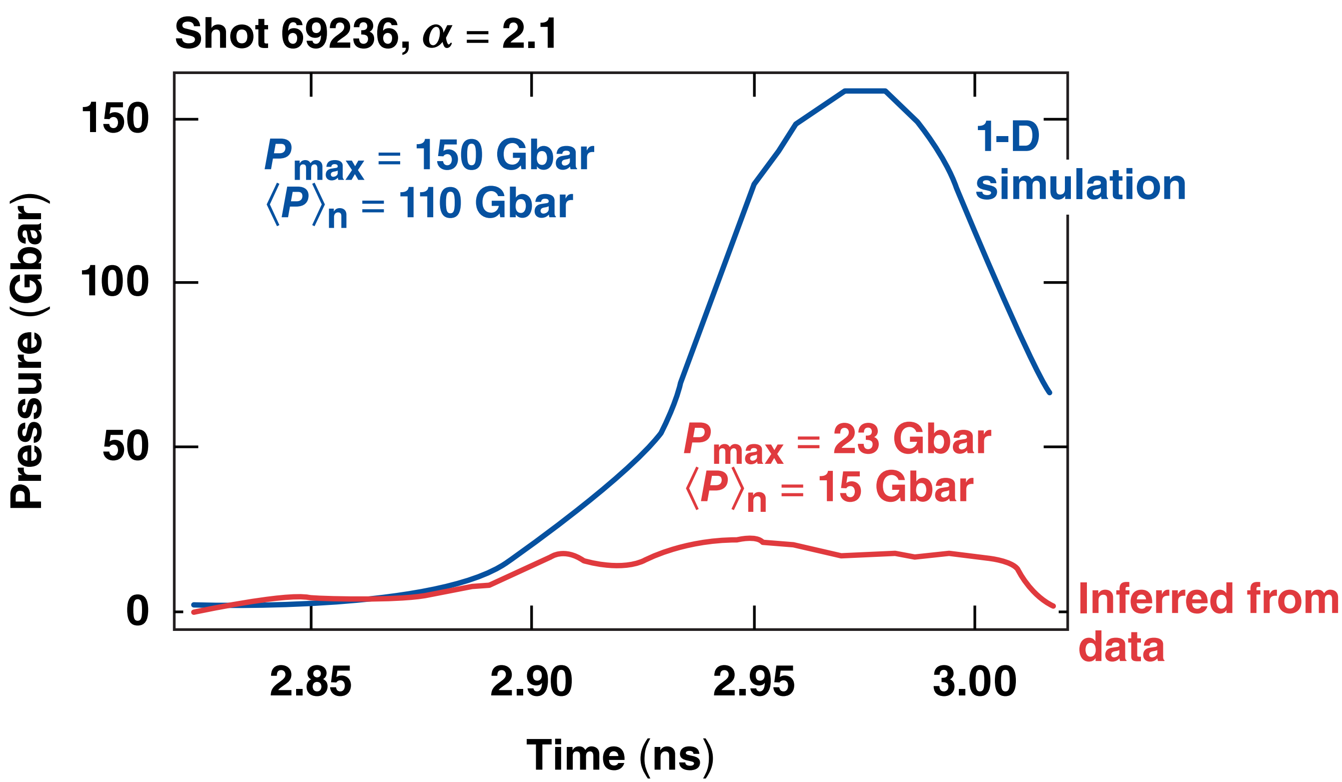

TC10958

The highest hot-spot pressure is achieved for α ~ 4 implosions at IFAR ~ 22

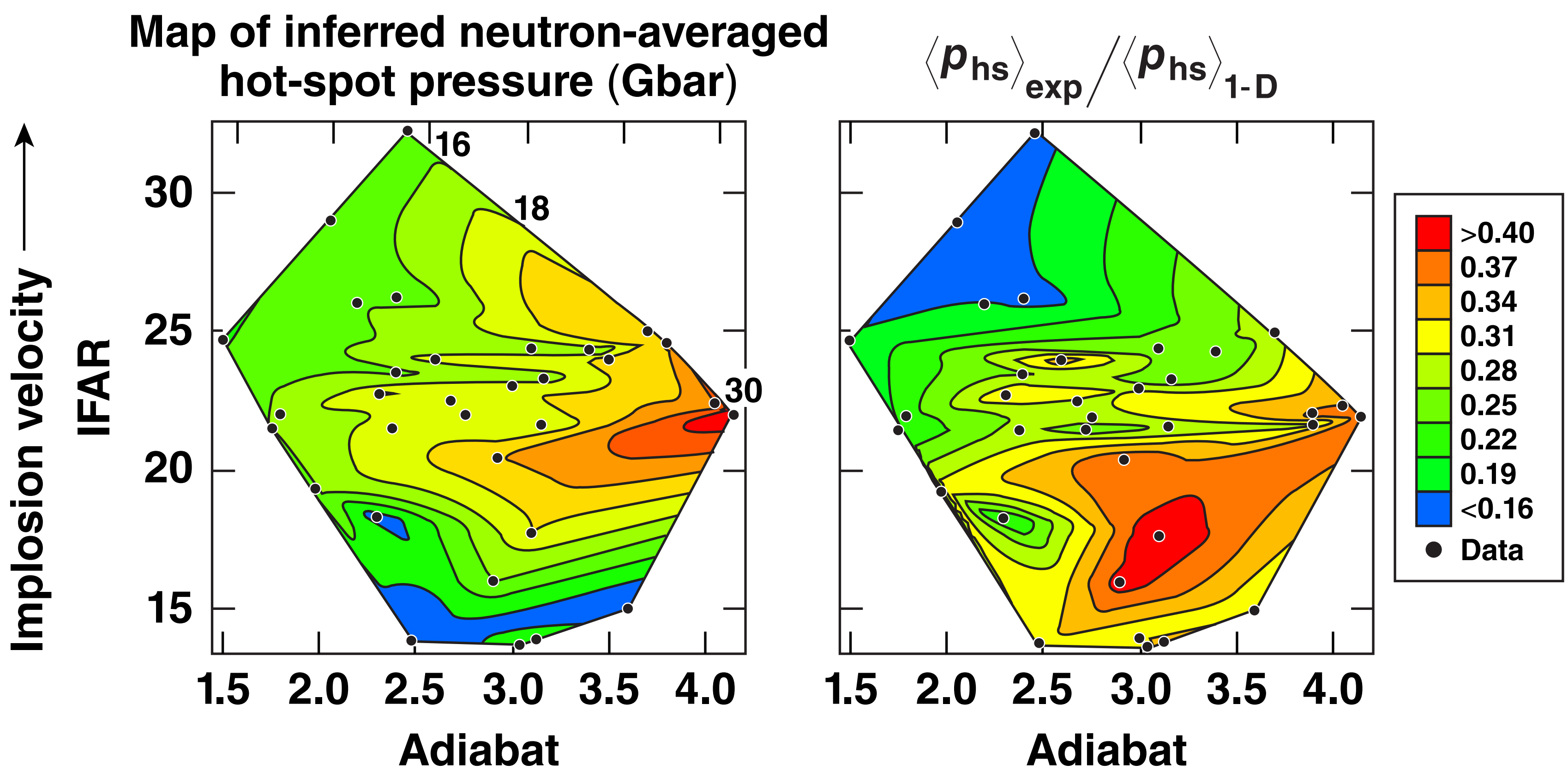

TC10959

Two-dimensional simulations for $\alpha \gtrsim 4$ implosions reproduce measured stagnation quantities

UR LLE

- Sources of nonuniformity included in simulation: laser imprint, ice roughness, power imbalance, and beam mistiming

Neutron temporal diagnostic (NTD) for shot 69514

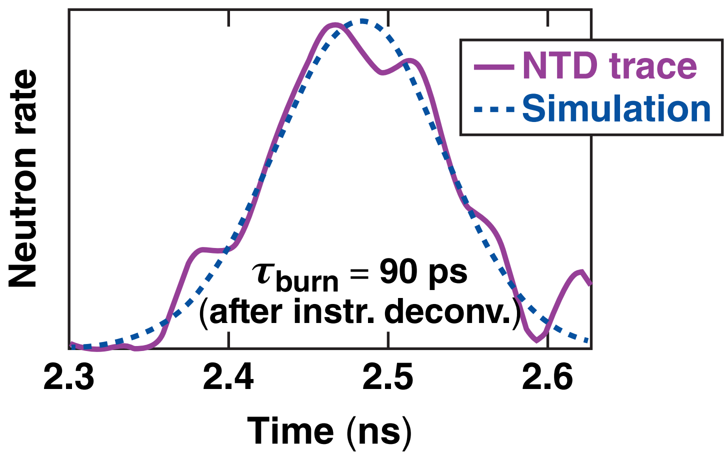

Measured self-emission profile for 69514: R_{17} = 25.2 μm

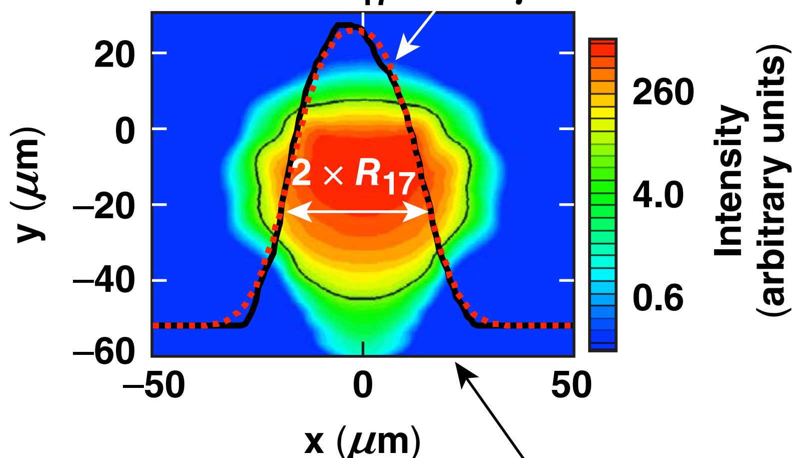

*SPECT3D** post-processed *DRACO* simulations

	Simulation	Experiment
Yield	3.9×10^{13}	3.0×10^{13}
T_i	3.7 keV	3.6 keV
ρR	0.18 g/cm^2	0.17 g/cm^2
R_{17}	24.4 μm	25.2 μm
P_{hs}	32 Gbar	30 Gbar

*Prism Computational Sciences, Inc., Madison, WI Report PCS-R-025, Ver. 2.1 (2001).

E22296i

2-D Simulations

Shell instability is the main candidate for performance degradation in low-adiabat implosions

- Simulations* include ~100 surface features, size: 5 to 20 μm in diameter, 0.5 to 1.0 μm in depth

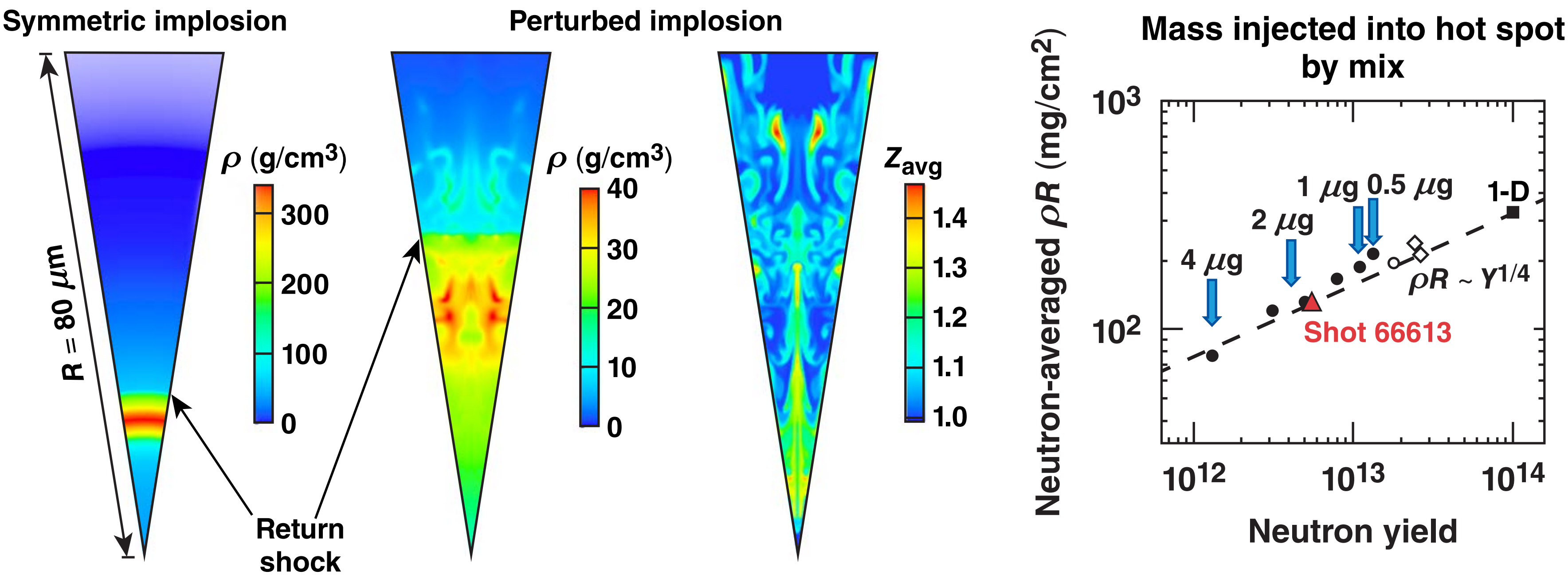

The main goal of these simulations is to identify a possible hydrodynamic scenario that explains the observations.

TC10308b

*I. V. Igumenshchev *et al*., Phys. Plasmas 20, 082703 (2013).

Hydrodynamic simulations including local defects match the evolution of hot-spot pressure and neutron rate

Shot 66613, $\alpha = 2$

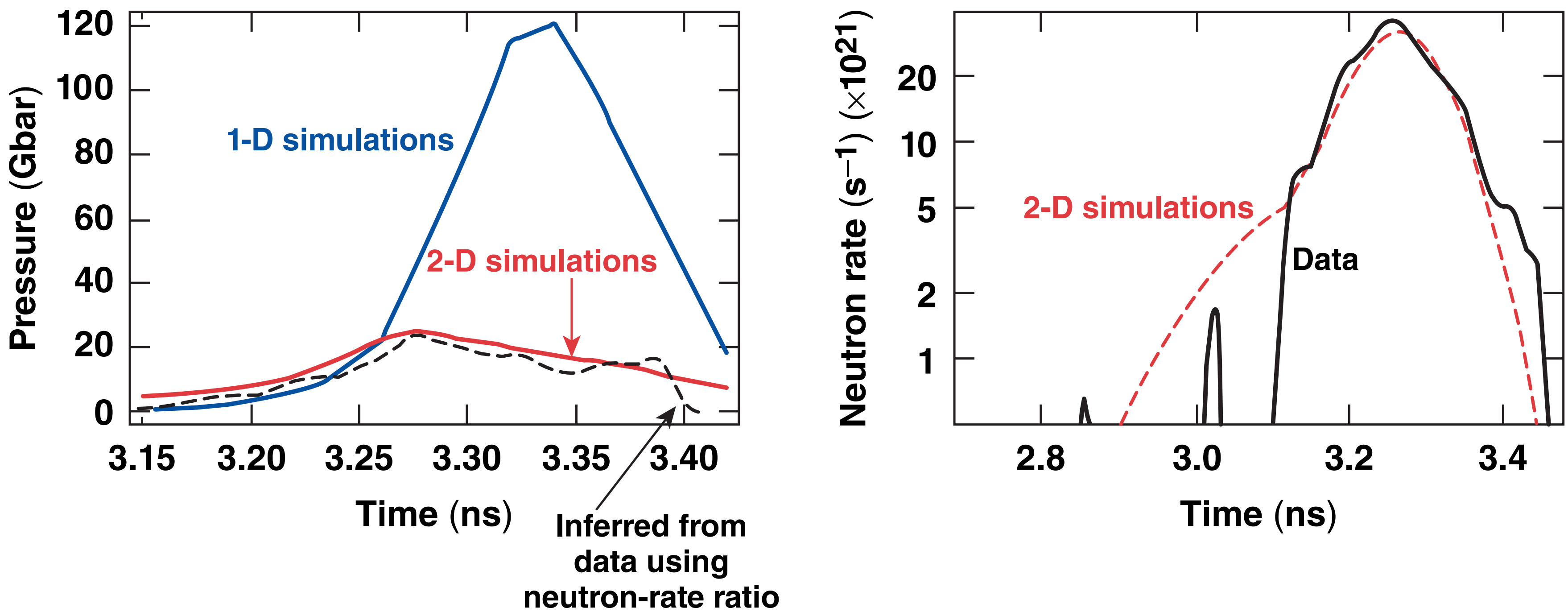

TC10990

Excessive vapor mass leads to a larger hot-spot radius at stagnation

UR LLE

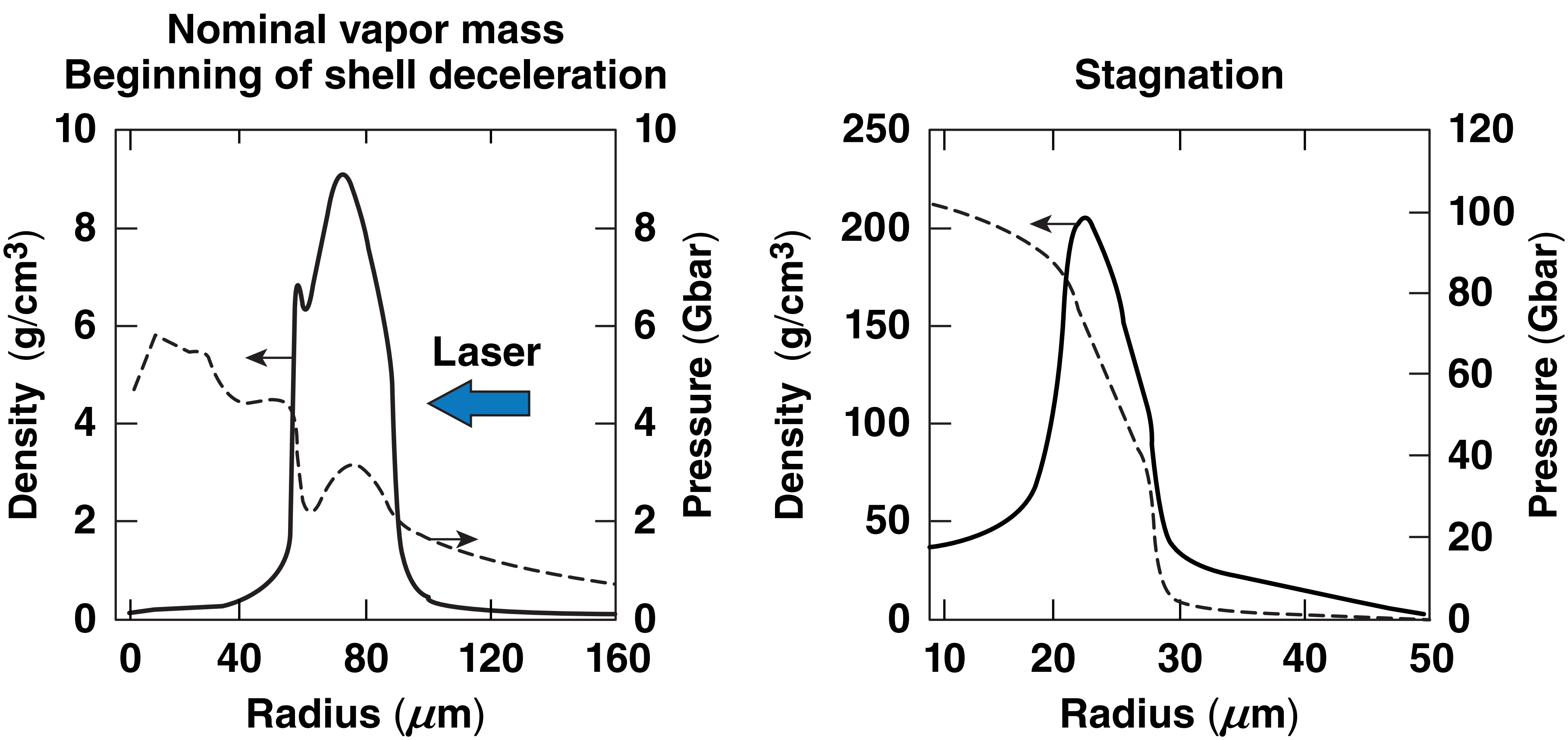

TC10991

Excessive vapor mass leads to a larger hot-spot radius at stagnation

- Fuel contamination and ablator-to-vapor mix contribute to larger vapor mass

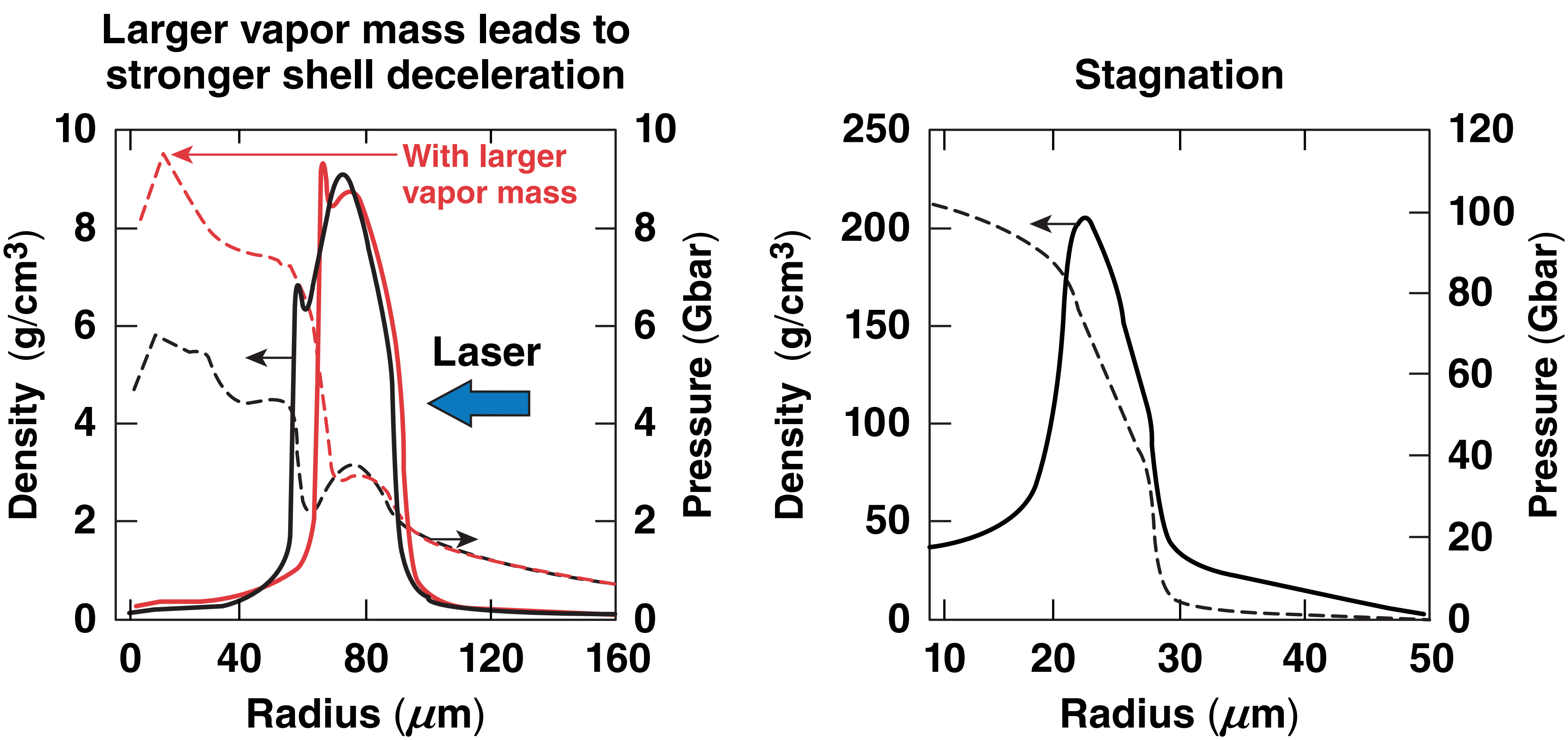

TC10991a

Excessive vapor mass leads to a larger hot-spot radius at stagnation

- Fuel contamination and ablator-to-vapor mix contribute to larger vapor mass

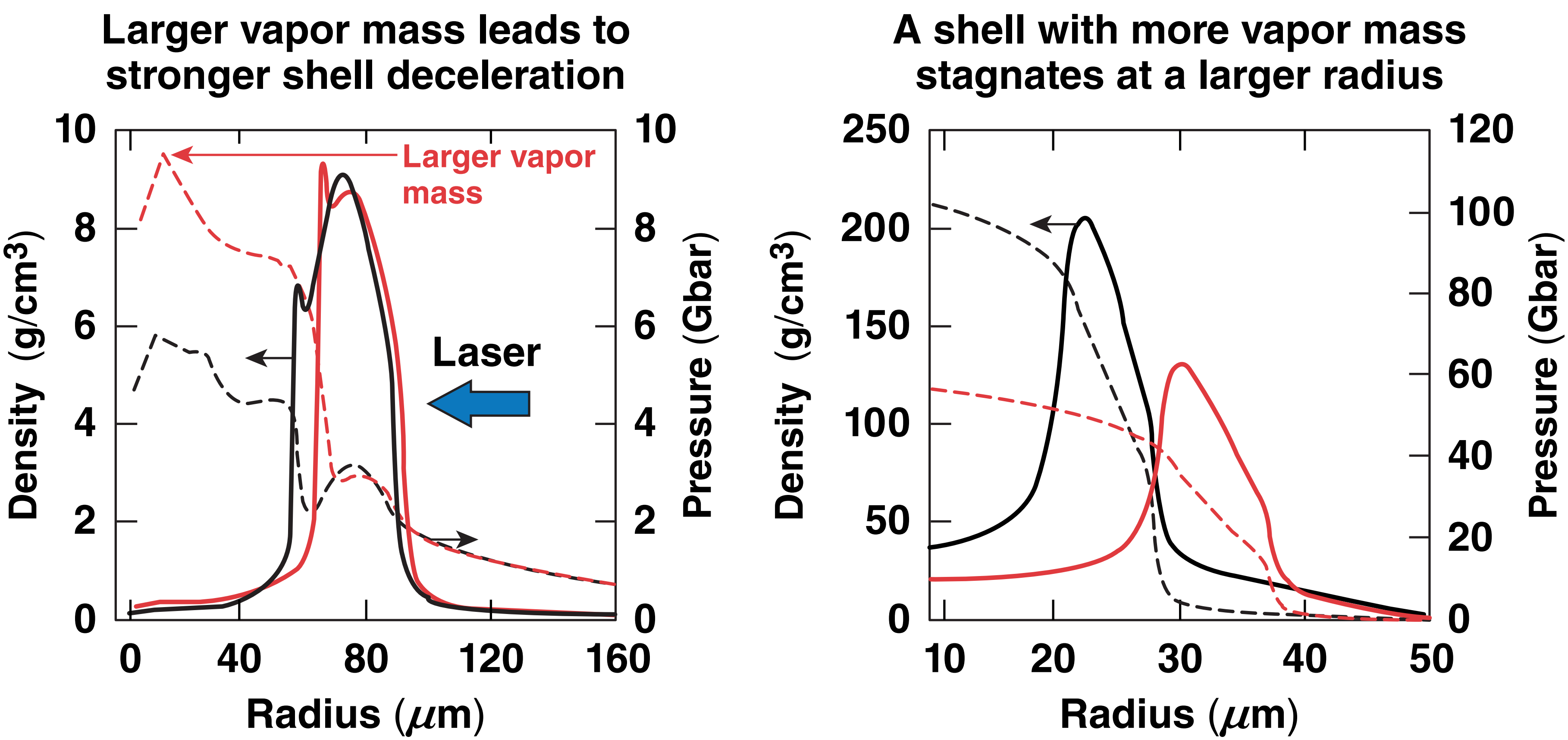

$$\rho R \sim \frac{\rho R_{max}}{\sqrt{1+\frac{m_{vapor}}{m_{norm}}}}, P_{hs} \sim \frac{P_{max}}{\left(1+\frac{m_{vapor}}{m_{norm}}\right)^{0.8}}$$

- For OMEGA targets: $m_{norm} = 0.1\ \mu g$
- Vapor mass increases to 2 μg because of mix in $\alpha < 2.5$ implosions

TC10991b

Reduced shell density contributes to degradation in hot-spot compression

UR LLE

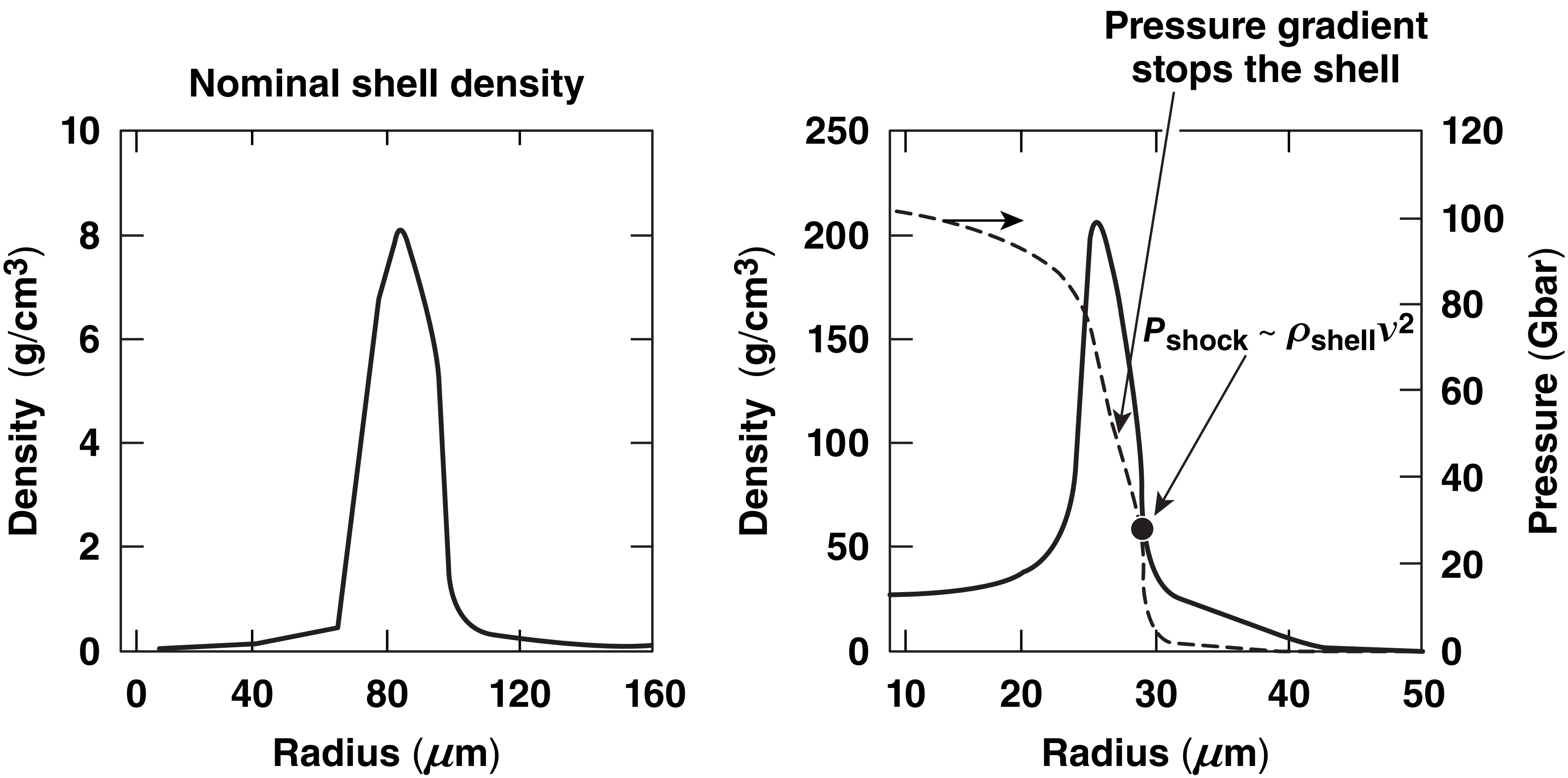

TC10992

Reduced shell density contributes to degradation in hot-spot compression

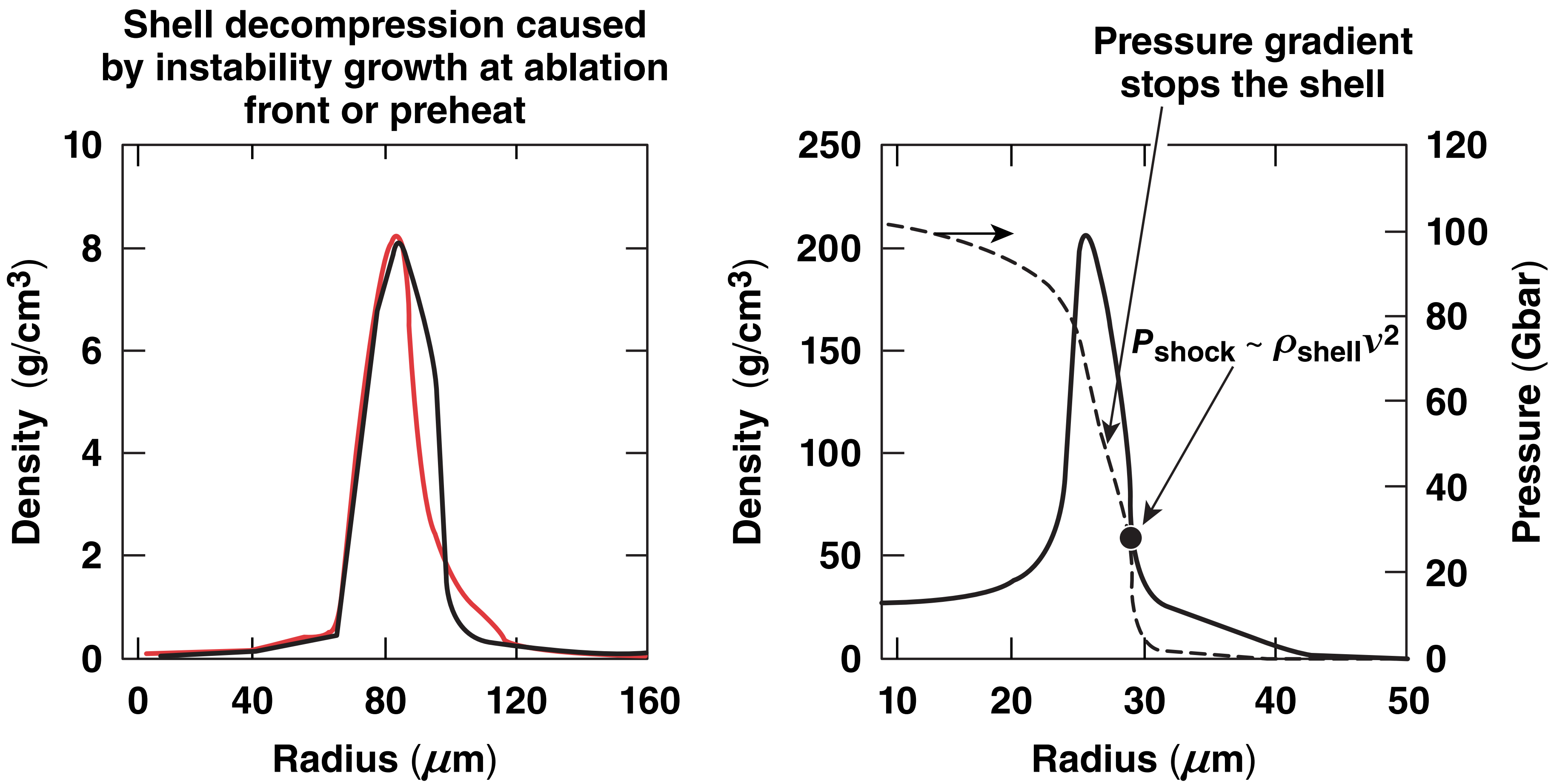

TC10992a

Reduced shell density contributes to degradation in hot-spot compression

Shell decompression caused by instability growth at ablation front or preheat

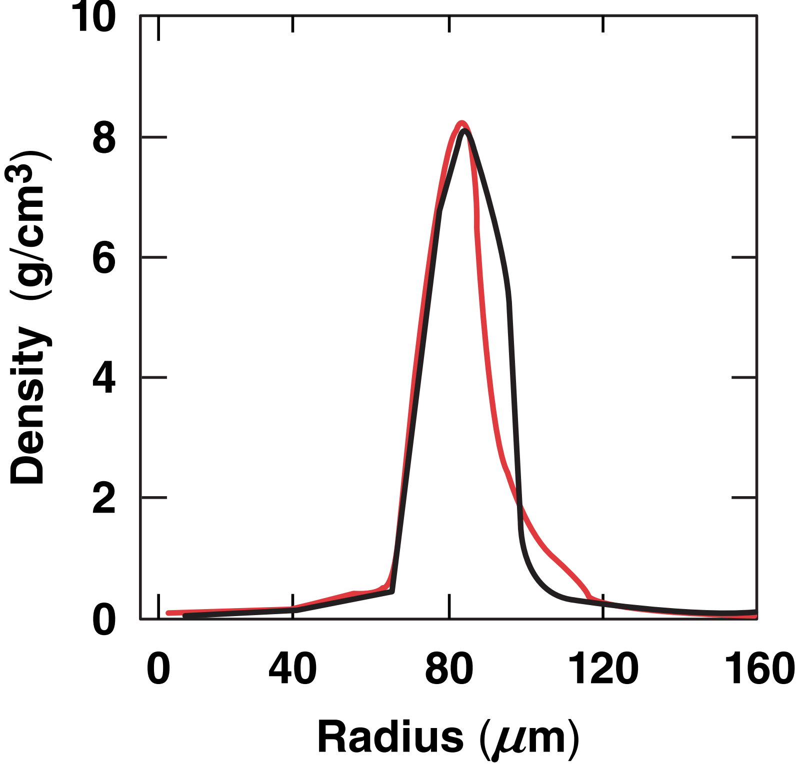

Pressure gradient stops the shell

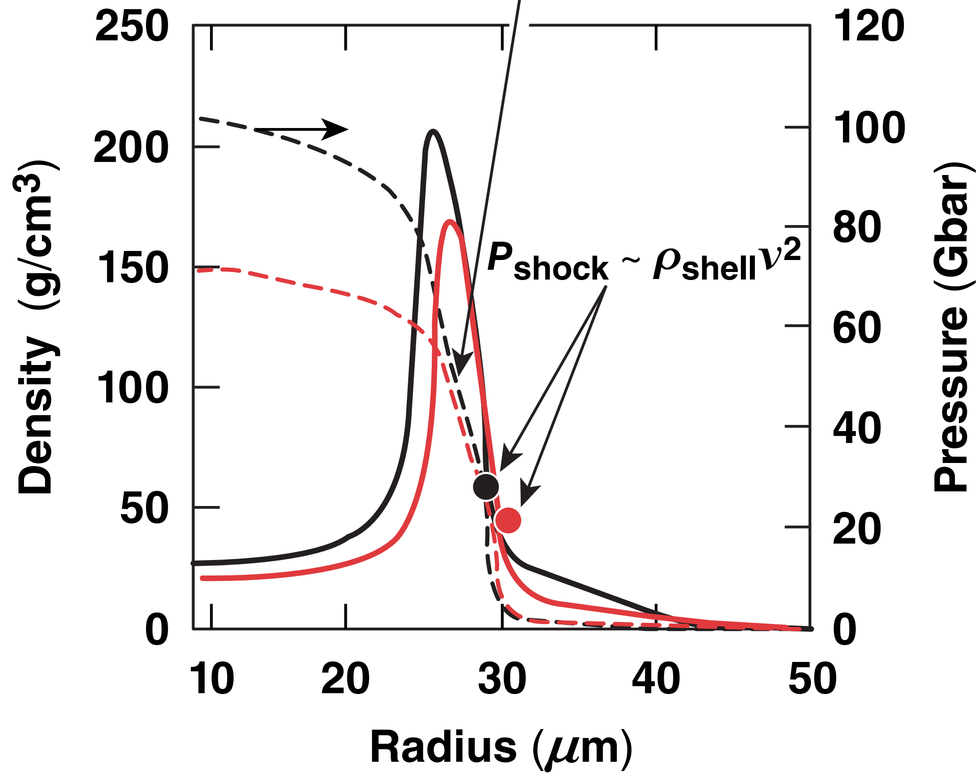

For smaller P_{shock}, lower P_{hs} stops the shell → larger stagnation hot-spot radius.

TC10992b

Target compression degradation caused by ablation-front mix depends on the fraction of shell mass overtaken by the shock at bang time

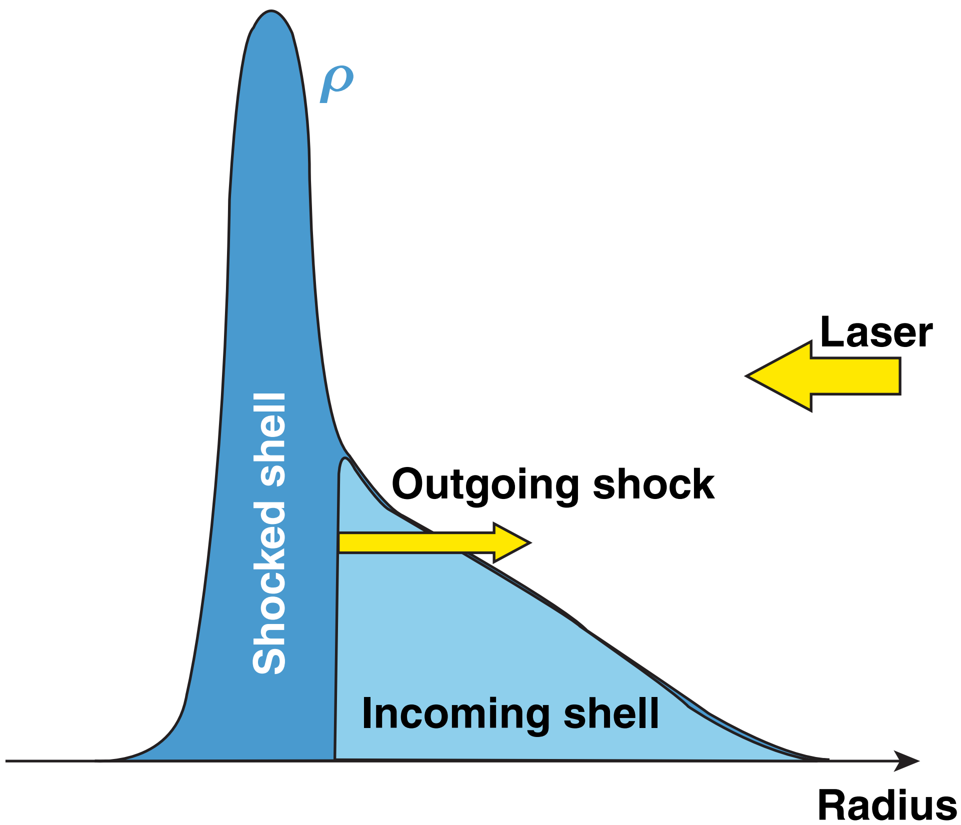

TC10993

Target compression degradation caused by ablation-front mix depends on the fraction of shell mass overtaken by the shock at bang time

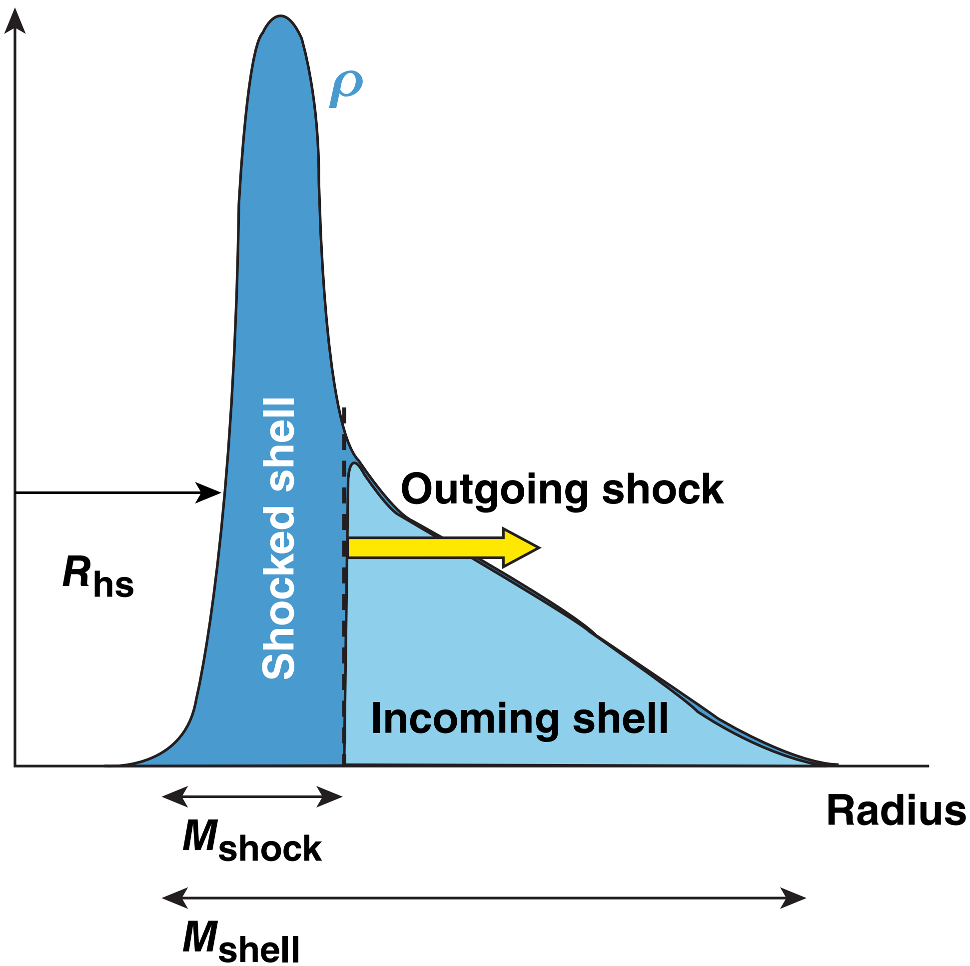

TC10993a

Target compression degradation caused by ablation-front mix depends on the fraction of shell mass overtaken by the shock at bang time

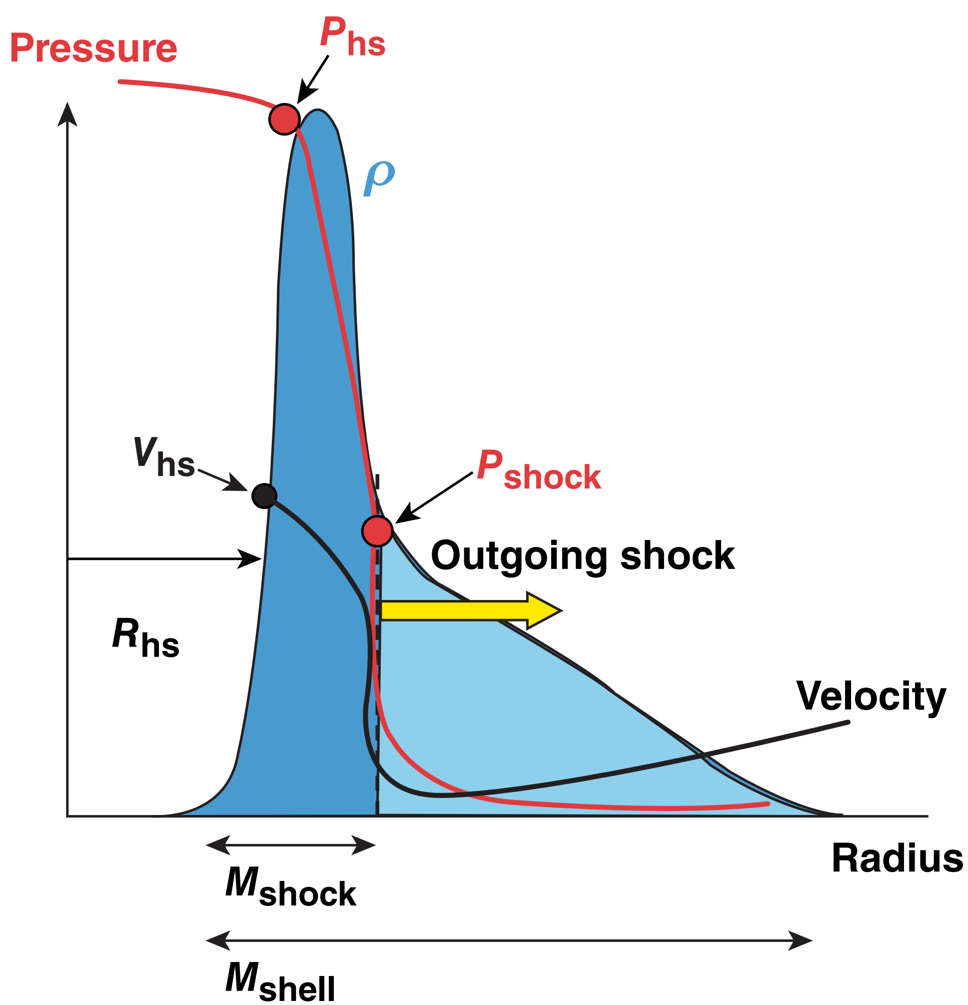

TC10993b

Degradation Mechanisms

Target compression degradation caused by ablation-front mix depends on the fraction of shell mass overtaken by the shock at bang time

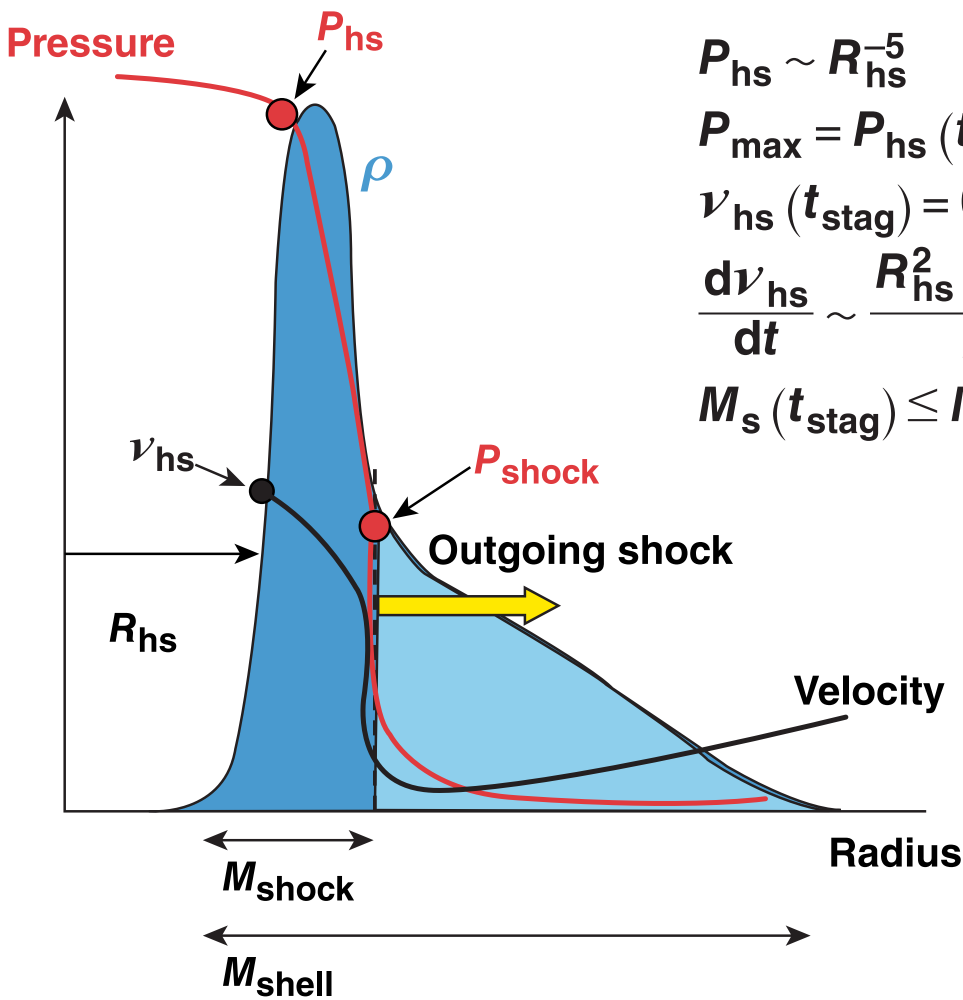

$$P_{hs} \sim R_{hs}^{-5}$$

$$P_{max} = P_{hs}\left(t_{stag}\right)$$

$$\nu_{hs}\left(t_{stag}\right) = 0$$

$$\frac{d\nu_{hs}}{dt} \sim \frac{R_{hs}^2\left(P_{hs} - P_{shock}\right)}{M_{shock}\left(t\right)}$$

$$M_s\left(t_{stag}\right) \le M_{shell}$$

TC10993c

Target compression degradation caused by ablation-front mix depends on the fraction of shell mass overtaken by the shock at bang time (continued)

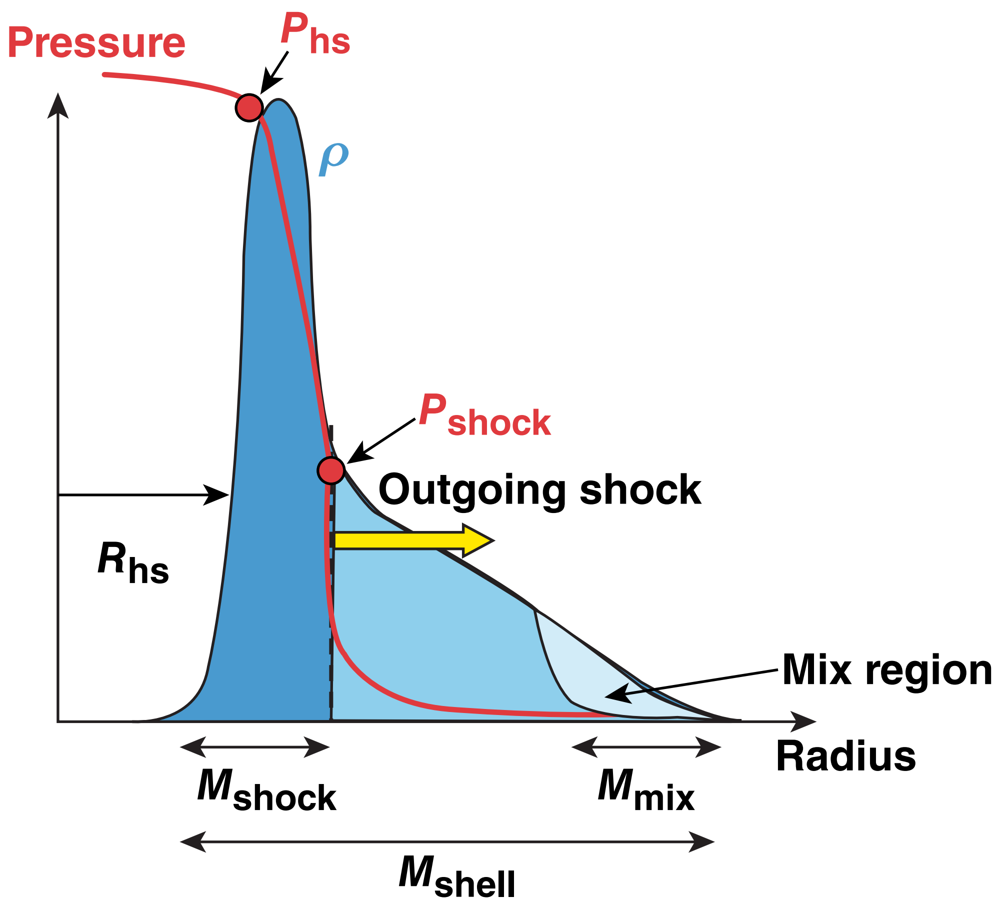

Target performance is not degraded if $M_{mix} < M_{shell} - M_{shock}(t_{stag}) = M_{unshocked}$.

TC10993d

Shocked-shell fraction at stagnation depends on implosion velocity, adiabat, and drive pressure

UR LLE

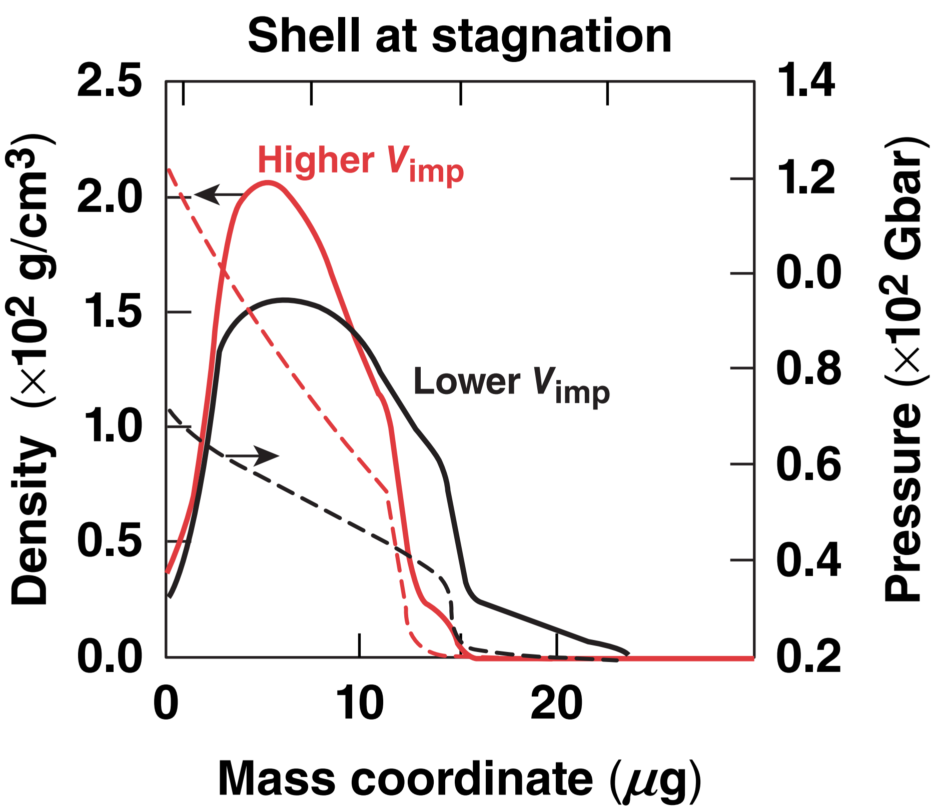

$$\frac{M_{shock}}{M_{shell}} \sim \frac{V_{imp}^{4/3}}{\alpha^{2/5} P_a^{4/15}}$$

TC10994

Shocked-shell fraction at stagnation depends on implosion velocity, adiabat, and drive pressure

UR LLE

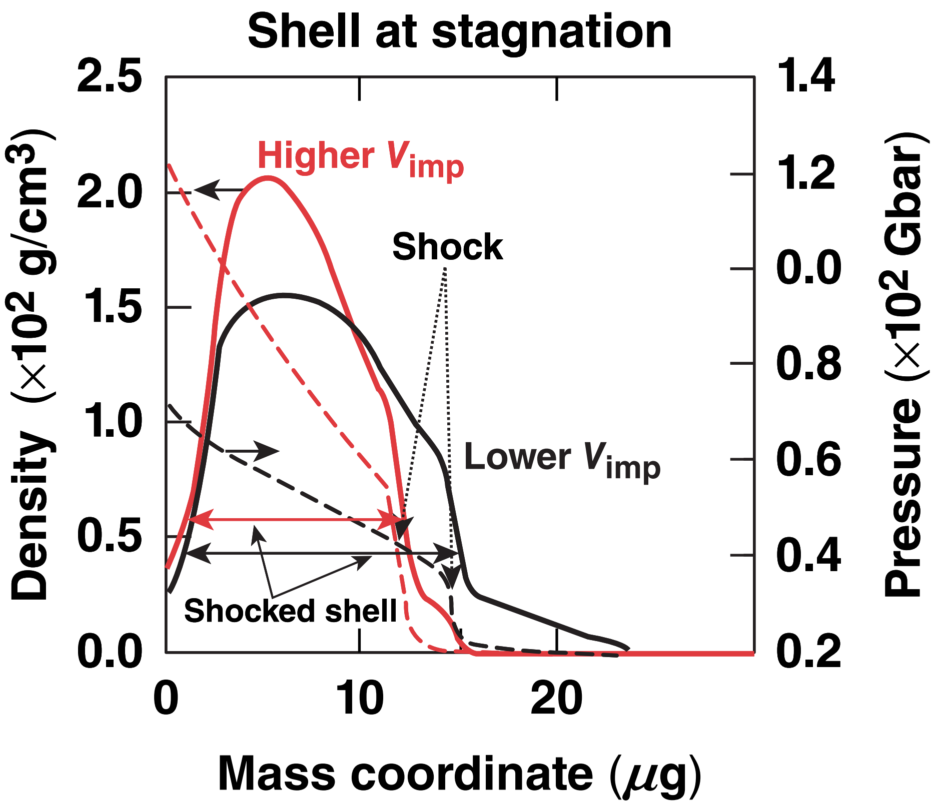

$$\frac{M_{shock}}{M_{shell}} \sim \frac{V_{imp}^{4/3}}{\alpha^{2/5} P_a^{4/15}}$$

TC10994a

Shocked-shell fraction at stagnation depends on implosion velocity, adiabat, and drive pressure

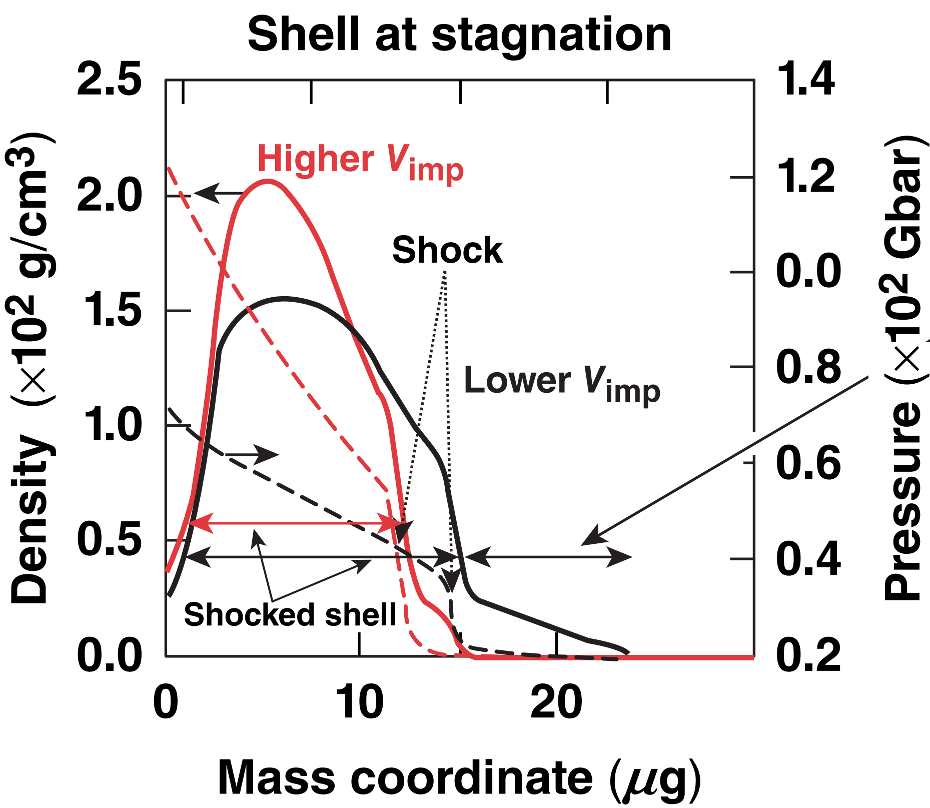

More unshocked mass, less sensitivity to Rayleigh–Taylor (RT) mix at ablation front

TC10994b

Reduction in peak areal density and pressure depends on the mass of the mix region relative to the unshocked mass

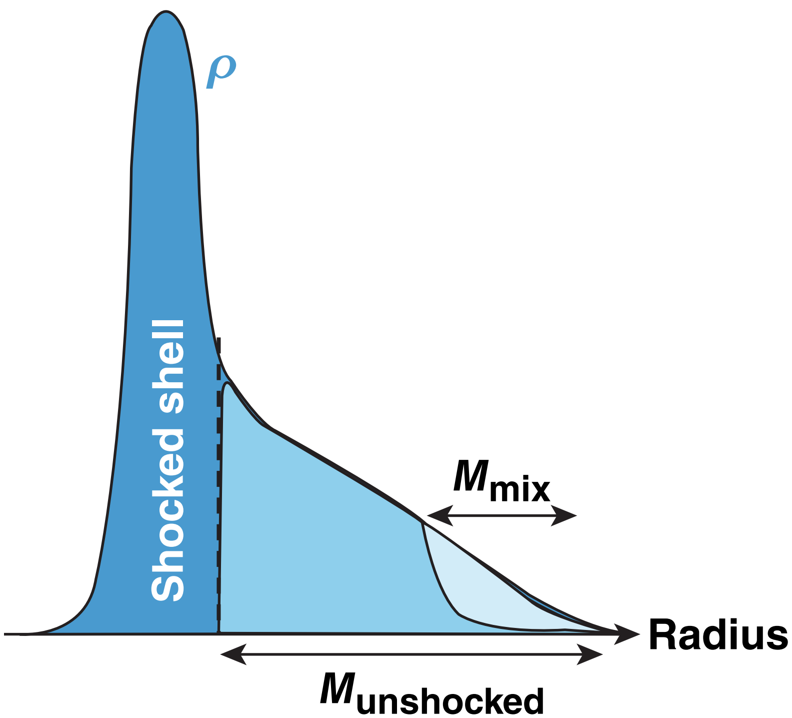

One-dimensional simulations with reduced density at the end of acceleration

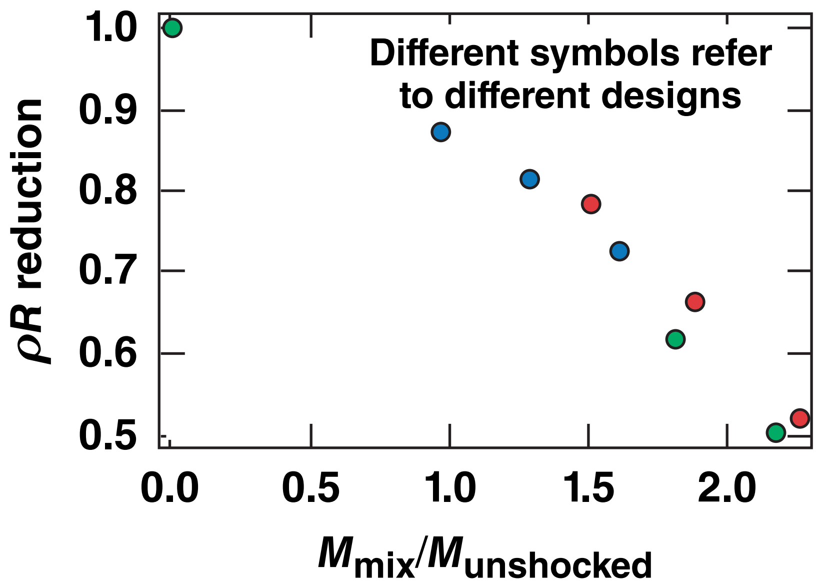

Target compression degradation is a strong function of unshocked mass at peak neutron production

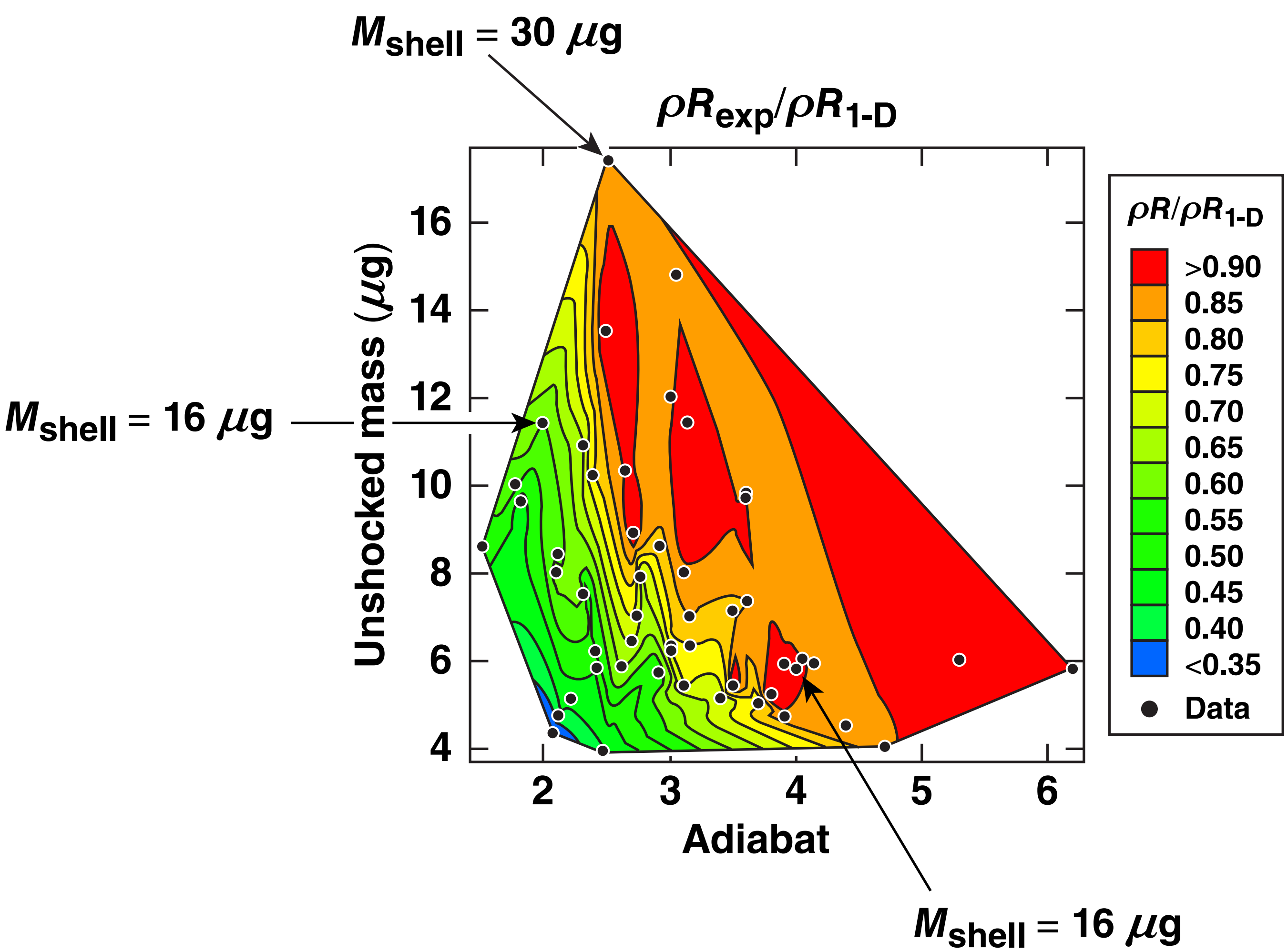

TC10996

Amount of RT mix at the ablation front can be inferred from the stability boundary

8 μg of shell is mixed at the ablation front because of a RT growth

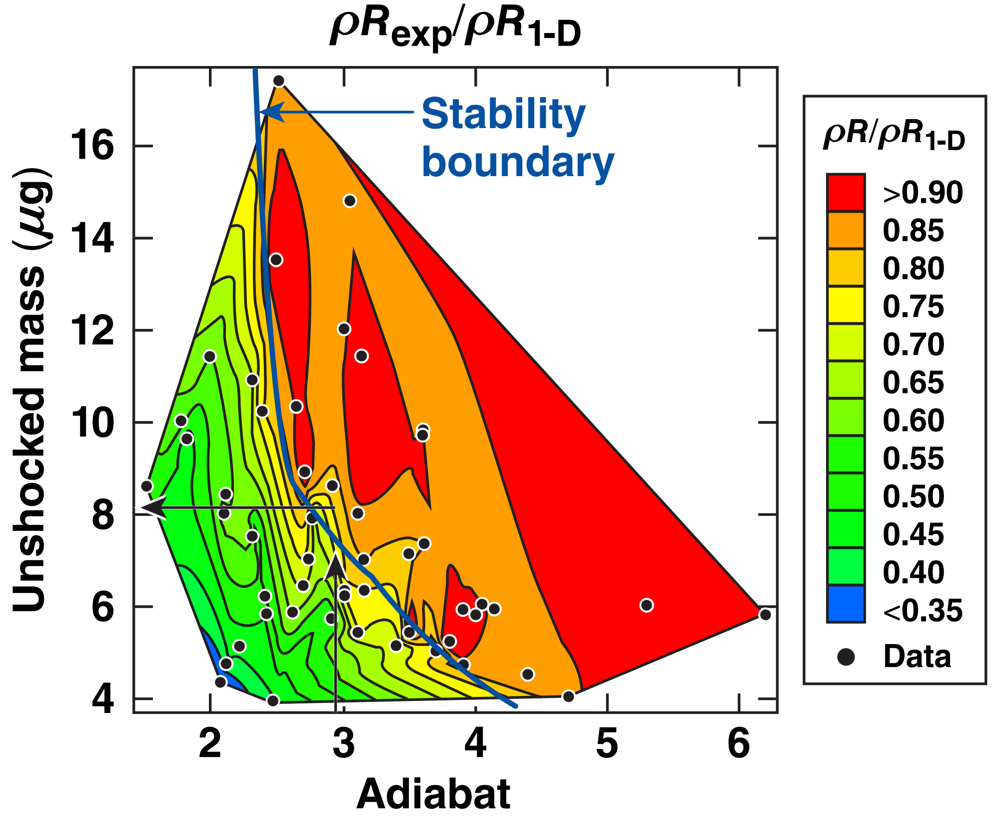

TC10996a

Significant mix of the ablator material into the hot-spot limits performance of α < 2.5 implosions

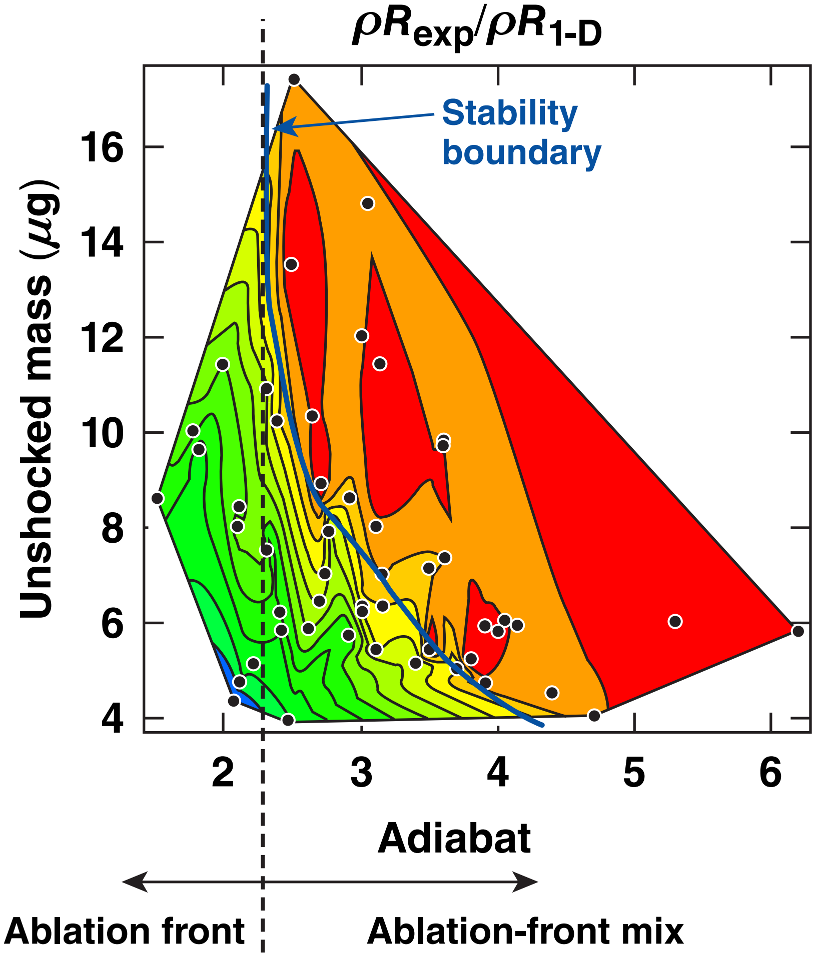

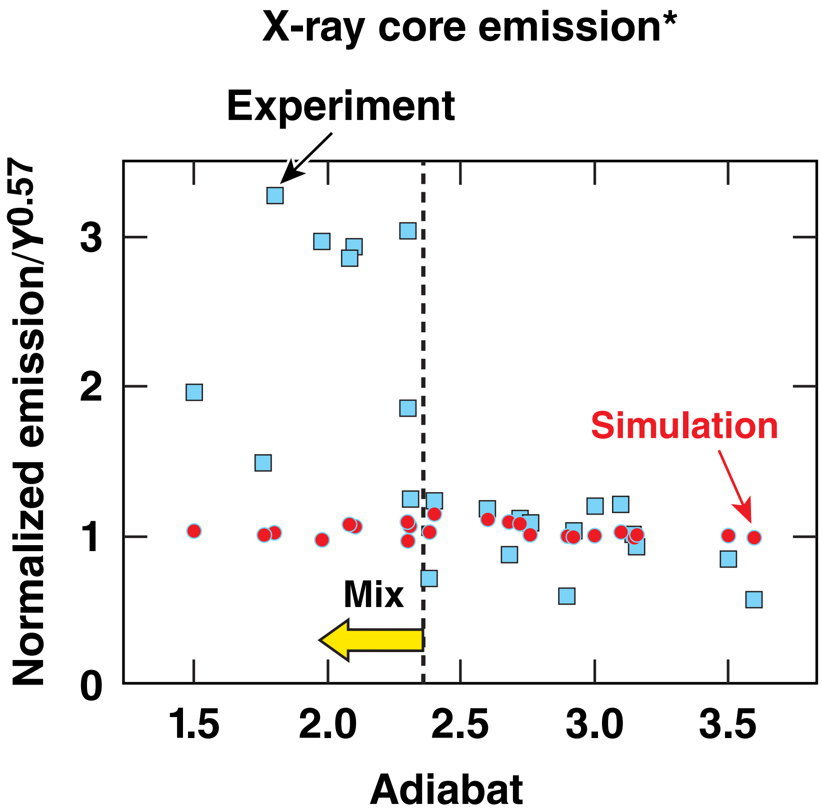

TC10996b

*T. C. Sangster *et al*., Phys. Plasmas 20, 056317 (2013).

Mitigating CBET* allows the shell and unshocked masses to be increased

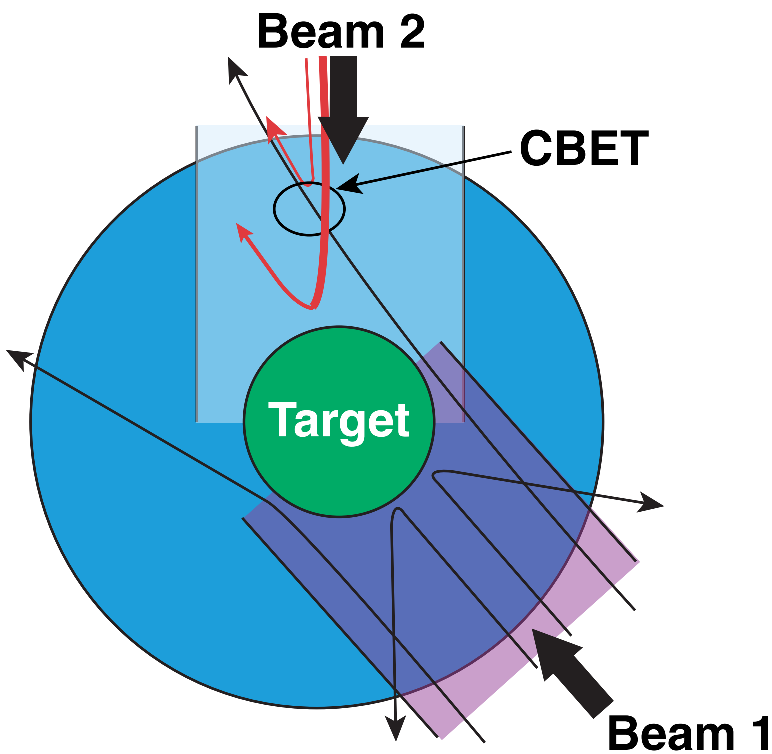

*I. V. Igumenshchev *et al*., Phys. Plasmas 17, 122708 (2010).

TC10997

Mitigating CBET* allows the shell and unshocked masses to increase

Using smaller beams at the main drive reduces CBET

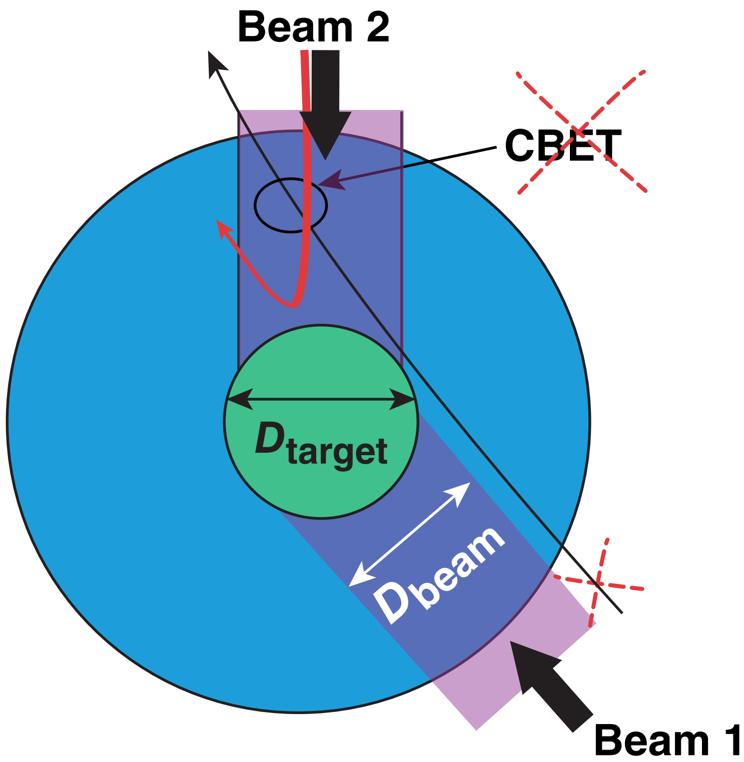

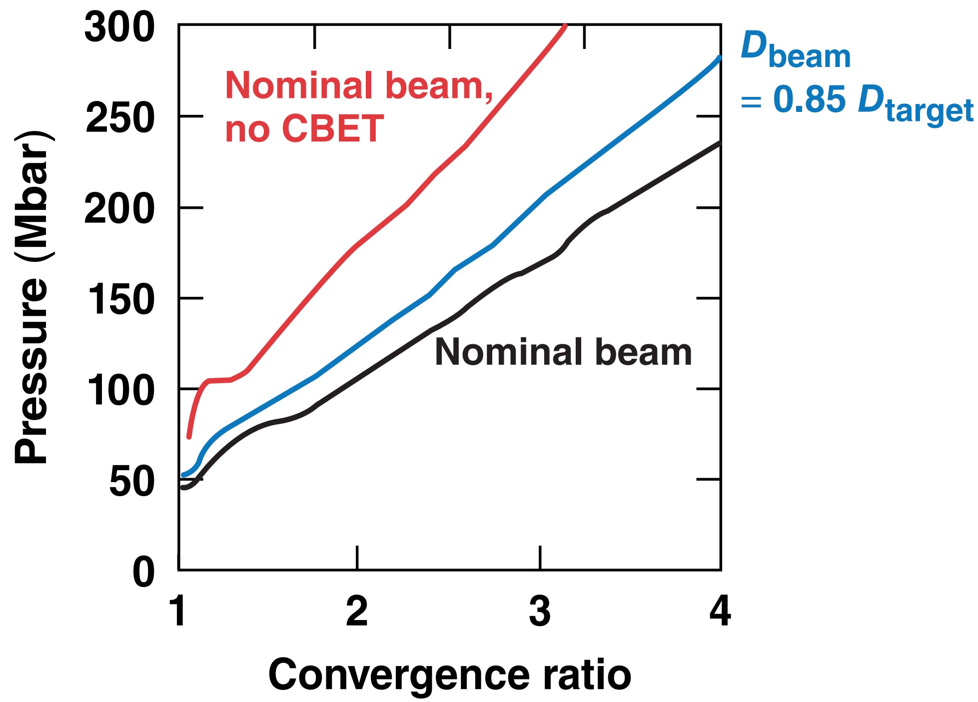

*I. V. Igumenshchev *et al.*, Phys. Plasmas 17, 122708 (2010).

TC10997a

Mitigating CBET makes it possible to drive more massive targets at a higher adiabat

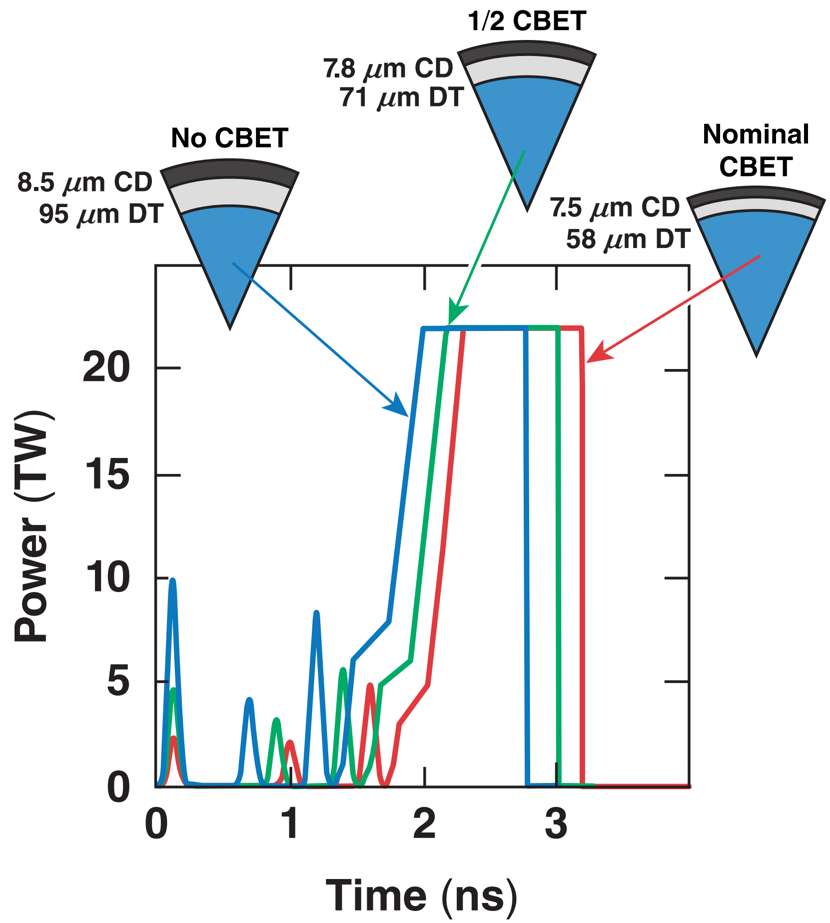

TC11092

Mitigating CBET is required to demonstrate ignition hydrodynamic scaling on OMEGA

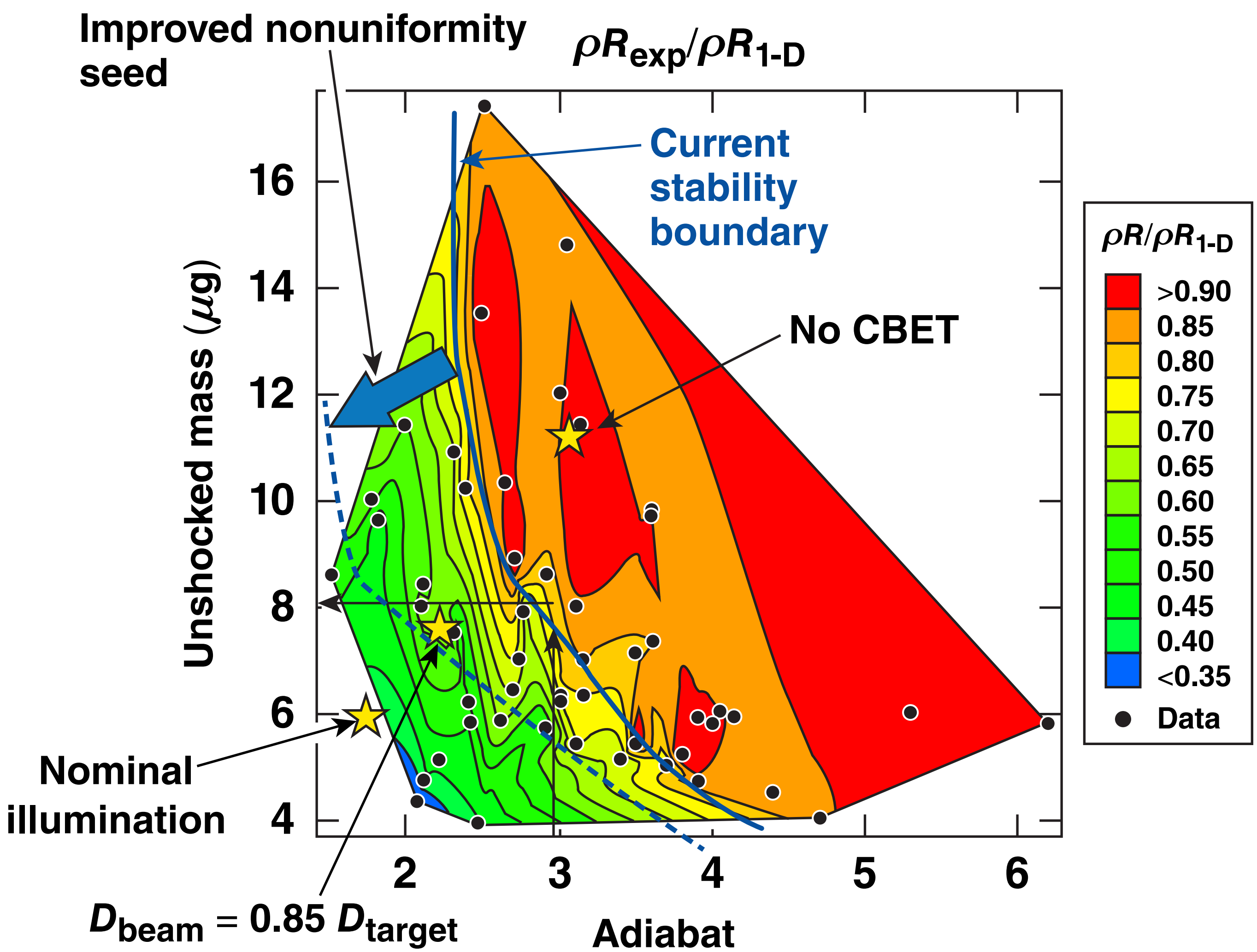

☆ Hydro-equivalent designs

- Ignition hydrodynamic-equivalent OMEGA implosions require $\rho R \sim 300$ mg/cm^2 and $V_{imp} \sim 3.7 \times 10^7$ cm/s

TC10998O

The performance degradation of OMEGA cryogenic implosions is understood in terms of unshocked shell mass at stagnation

- Yields in excess of 3.4×10^{13} [yield-over-clean (YOC) ~ 35%] and ion temperatures up to 4 keV were measured in cryogenic implosions with $V_{imp} \sim 3.8 \times 10^7$ cm/s
- Performance degradation in moderate-adiabat ($\alpha \sim 4$) implosions is fully understood by 2-D *DRACO* simulations
- Shells in lower-adiabat implosions ($\alpha \sim 2.5$) break up during acceleration, leading to an increased hot-spot mass and reduced convergence
- The unshocked mass at peak compression determines the impact of the ablator mix

Improving shell stability and mitigating cross-beam energy transfer (CBET) are required to demonstrate ignition hydrodynamic scaling on OMEGA.

TC10247c